4

Kinetics and Mechanisms of Soil Chemical Reactions

Donald L. Sparks
University of Delaware

4.1 Introduction

Since its inception in the mid 1850s, soil chemistry has focused on the macroscopic, equilibrium aspects of soil chemical reactions and processes. From these studies, much was learned about important soil chemical processes including sorption, desorption, precipitation, complexation, dissolution and oxidation/reduction. However, such investigations do not convey information on reaction rates or reaction mechanisms. In the past two decades, as concerns and interests about soil and water quality have increased, soil and environmental chemists, environmental and chemical engineers and geochemists have increasingly realized that reactions in subsurface environments are time dependent. Thus, to accurately predict the fate, mobility, speciation, and bioavailability of environmentally important plant nutrients, trace elements, radionuclides, and organic chemicals in soils, one must understand the kinetics and mechanisms of the reactions.

While major progress has been made in better understanding the kinetics of soil chemical processes, much uncertainty remains. In part, this is due to the complex, heterogeneous nature of natural materials such as soils. However, with development of kinetic techniques that can be used to measure a wide range of time scales, time-dependent models that can describe both chemical reaction and mass transfer processes, and the employment of state-of-the-art *in situ* spectroscopic and microscopic surface techniques in combination with rate studies, major advances are being made in understanding the kinetics and mechanisms of soil chemical reactions. Arguably, this will be a major leitmotif in soil chemistry research for decades to come.

In this review, the application of chemical kinetics to heterogeneous systems such as soils and soil components (clay minerals, organic matter, and humic substances), with emphasis on sorption/release processes will be discussed. A critical review of kinetic models that can be used to describe reaction rates on heterogeneous surfaces will be covered. The review will also present discussions on the rates of important soil chemical reactions and processes including inorganic and organic sorption/desorption, dissolution and redox. For additional details on these topics and other aspects of kinetics of soil chemical and geochemical processes, the reader should consult a number of recent books and

monographs (Sparks, 1989; Sparks and Suarez, 1991; Stumm, 1992; Schwarzenbach et al., 1993; Sposito, 1994; Sparks, 1995).

4.2 Time Scales of Soil Chemical Processes

A variety of chemical reactions occur in soils and often in combination with one another. Reaction time scales can vary from microseconds and milliseconds for many ion association and some ion exchange and sorption reactions to years for many mineral solution and mineral crystallization phenomena and for some sorption/release reactions (Fig. 4.1). Ion association reactions include ion pairing, inner and outersphere complexation, and chelation in solution. Gas-water reactions involve gaseous exchange across the air-liquid interface. Ion exchange reactions occur when cations and anions are adsorbed (outersphere complexation) and desorbed from soil surfaces by electrostatic attractive forces. Ion exchange reactions are reversible and stoichiometric. Sorption reactions can involve adsorption processes including partitioning, outersphere and innersphere complexation, and multinuclear complexation (e.g., surface precipitation). Mineral-solution reactions include precipitation/dissolution of minerals, and coprecipitation reactions in which small constituents become a part of mineral structures (Sparks, 1989; Amacher, 1991).

The type of soil component can drastically affect the reaction rate. For example, sorption reactions are often more rapid on clay minerals such as kaolinite and smectites than on vermiculitic and micaceous minerals. This is in large part due to the availability of sites for sorption. For example, kaolinite has readily available planar external sites and smectites have primarily internal sites that are also quite available for retention of sorbates. Thus, sorption reactions on these soil constituents are often quite rapid, even occurring on time scales of seconds and milliseconds (Sparks, 1989).

On the other hand, vermiculite and micas have multiple sites for retention of metals and organics, including planar, edge, and interlayer sites, with some of the latter sites being partially to totally collapsed. Consequently, sorption and desorption reactions on these sites can be slow, tortuous, and mass transfer controlled. Often, an apparent equilibrium may not be reached even after several days or weeks. Thus, with vermiculite and mica, sorption can involve two to three different reaction rates: high rates on external sites, intermediate rates on edge sites, and low rates on interlayer sites (Jardine and Sparks, 1984; Comans and Hockley, 1992).

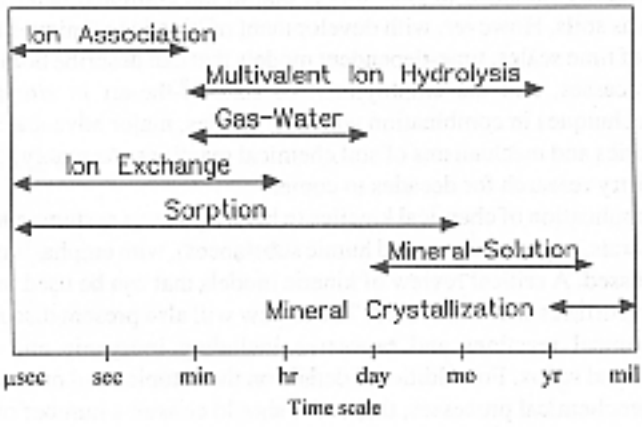

Fig. 4.1 Time ranges required to attain equilibrium by different types of reactions in soil environments [Reprinted from Amacher, 1991. Soil Sci. Soc. Am. Spec Pub. 27 with permission of the Soil Science Society of America]

Metal sorption reactions on oxides, hydroxides, and humic substances depend on the type of surface and metal being studied, but the chemical reaction rate appears to be rapid. For example, chemical reaction rates of metals and oxyanions on goethite occurred on millisecond time scales (Zhang and Sparks, 1989, 1990 a,b; Grossl et al., 1994; Grossl et al., 1997). Half-times for divalent Pb, Cu, and Zn sorption on peat ranged from 5 to 15 s (Bunzl et al., 1976). A number of studies have shown that heavy metal sorption on oxides (Bruemmer et al., 1988; Ainsworth et al., 1994; Scheidegger et al., 1996a, 1998) and clay minerals (Lövgren et al., 1990) increase with longer residence times. The mechanism for these lower reaction rates is not well understood, but has been ascribed to diffusion phenomena, sites of lower reactivity, and surface nucleation/precipitation (Scheidegger and Sparks, 1996b; Sparks, 1998, 1999). Recent findings on slow metal retention rates and mechanisms at the mineral/water interface will be discussed later.

Sorption/desorption of metals and organic chemicals on soils is often very slow which has been attributed to diffusion into micropores of inorganic minerals and into humic substances, retention on sites of varying reactivity, and surface nucleation/precipitation (Scheidegger and Sparks, 1996b; Sparks, 1997, 1999). These reactions will be discussed in more detail later.

4.3 Application of Chemical Kinetics to Heterogeneous Surfaces

The study of chemical kinetics, even in homogeneous systems, is complex and often arduous. When one attempts to study the kinetics of reactions in heterogeneous systems such as soils, sediments and even soil components such as clay minerals, hydrous oxides, and humic substances, the difficulties are greatly magnified. This is largely due to the complexity of soils which are made up of a mixture of inorganic and organic components. These components often interact with each other and display different types of sites with various reactivities for inorganic and organic sorptives. Moreover, the variety of particle sizes and porosities in soils and sediments further adds to their heterogeneity. In most cases, both chemical kinetics and multiple transport processes are occurring simultaneously. Thus, the determination of chemical kinetics, which can be defined as "the investigation of rates of chemical reactions and of the molecular processes by which reactions occur where transport is not limiting" (Gardiner, 1969) is extremely difficult, if not impossible, in heterogeneous systems. In these systems, one is studying kinetics, which is a generic term referring to time dependent or nonequilibrium processes. Thus, apparent and non-mechanistic rate laws and rate parameters are determined (Skopp, 1986; Sparks, 1989).

4.3.1 Rate Limiting Steps

Both transport and chemical reaction processes can affect the reaction rates in the subsurface environment. Transport processes include (Aharoni and Sparks, 1991): (1) transport in the solution phase; (2) transport across a liquid film at the particle/liquid interface (film diffusion [FD]); (3) transport in liquid filled macropores (> 2 nm), all of which are nonactivated diffusion processes and occur in mobile regions; (4) particle diffusion (PD) processes which include diffusion of sorbate occluded in micropores (< 2 nm) (pore diffusion) and along pore wall surfaces (surface diffusion); and (5) diffusion processes in the bulk of the solid, all of which are activated diffusion processes (Fig. 4.2). Pore and surface diffusion within the immediate region can be referred to as interaggregate (interparticle) diffusion while that in the solid is intraaggregate diffusion. The actual chemical reaction (CR) at the surface, for example, adsorption, is usually instantaneous. The slowest of the CR and transport processes is rate limiting.

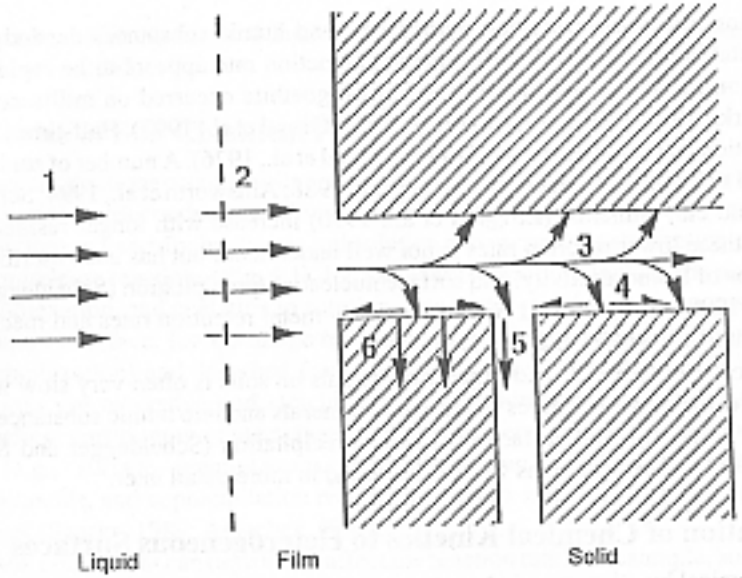

Fig. 4.2 Transport processes in solid-liquid soil reactions–nonactivated processes: (1) transport in the soil solution, (2) transport across a liquid film at the solid-liquid interface, (3) transport in a liquid-filled macropore; activated processes, (4) diffusion of a sorbate at the surface of the solid, (5) diffusion of a sorbate occluded in a micropore, (6) diffusion in the bulk of the solid [Reprinted from Aharoni and Sparks, 1991. Soil Sci. Soc. Am. Spec Pub. 27 with permission of the Soil Science Society of America]

4.3.2 Rate Laws

There are two important reasons for investigating the rates of soil chemical processes (Sparks, 1989,1995,1998, 1999): (1) to determine how rapidly reactions attain equilibrium, and (2) to infer information on reaction mechanisms. One of the most important aspects of chemical kinetics is the establishment of a rate equation or law. By definition, a rate law is a differential equation. For the following reaction (Bunnett, 1986; Sparks, 1989, 1995, 1998, 1999):

$$aA + bB \rightarrow yY + zZ \qquad [4.1]$$

the rate is proportional to some power of the concentrations of reactants A and B and/or other species (C, D, etc.) in the system and a, b, y, and z are stoichiometric coefficients and are assumed to be equal to one in the discussion that follows on rate laws. The power to which the concentration is raised may equal zero (i.e., the rate is independent of that concentration), even for reactant A or B. Rates are expressed as a decrease in reactant concentration or an increase in product concentration per unit time. Thus, the rate of conversion of reactant A above, which has a concentration $[A]$ at any time t, is $(-d[A]/(dt))$ while the rate with regard to product Y having a concentration $[Y]$ at time t is $(d[Y]/(dt))$.

The rate expression for Equation [4.1] is therefore,

$$\left|d[Y]/dt\right| = \left|-d[A]/dt\right| = k[A]^{\alpha}[B]^{\beta} \qquad [4.2]$$

where k is the rate constant and α and β are the orders of the reaction with respect to reactants A and B, respectively, and can be referred to as a partial orders for the total reaction. These orders are experimentally determined and not necessarily integral numbers. The sum of all the partial orders (α, β) is the overall order (n) of the total reaction and may be expressed as:

$$n = \alpha + \beta + \ldots \quad [4.3]$$

Once the values of α, β, etc., are determined experimentally, the rate law is defined. Reaction order provides only information about the manner in which rate depends on concentration. Order does not mean the same as molecularity which concerns the number of reactant particles (atoms, molecules, free radicals, or ions) entering into an elementary reaction. One can define an elementary reaction as one in which no reaction intermediates have been detected, or need to be postulated to describe the chemical reaction on a molecular scale. An elementary reaction is assumed to occur in a single step and to pass through a single transition state (Bunnett, 1986).

To demonstrate that a reaction is elementary, one can use experimental conditions that are different from those employed in determining the reaction rate law. For example, if one conducted kinetic studies using a flow technique with set steady-state flow rates, one could see if reaction rate and rate constants changed with flow rate. If they did, one would not be determining mechanistic rate laws (see definition below).

Rate laws serve three purposes: (1) they assist one in predicting the reaction rate; (2) mechanisms can be proposed; and (3) reaction orders can be ascertained. There are four types of rate laws that can be determined for soil chemical processes (Skopp, 1986): mechanistic, apparent, transport with apparent, and transport with mechanistic. Mechanistic rate laws assume that only chemical kinetics are operational and transport phenomena are not occurring. Consequently, it is difficult to determine mechanistic rate laws for most soil chemical systems due to the heterogeneity of the system caused by different particle sizes, porosities, and types of retention sites. There is evidence that with some kinetic studies, using chemical relaxation techniques (Sparks, 1989; Sparks and Zhang, 1991) and pure systems (e.g., clay minerals, oxides), mechanistic rate laws are determined or closely approximated since the agreement between equilibrium constants calculated from both kinetic and equilibrium studies are comparable (Hachiya et al., 1984; Tang and Sparks, 1993).

Since natural materials are heterogeneous and transport processes often affect the reaction rate, apparent rate laws are usually determined for such systems. Apparent rate laws include both chemical kinetics and transport-controlled processes. Thus, soil structure, stirring, mixing, and flow rate all would affect the kinetics. Transport with apparent rate laws emphasize transport limited phenomena. One often assumes first order or zero order reactions (see discussion below on reaction order). In determining transport with mechanistic rate laws, one attempts to describe simultaneously transport-controlled and chemical kinetics phenomena. One is thus trying to explain accurately both the chemistry and physics of the system.

4.3.3 Determination of Reaction Order and Rate Constants/Coefficients

There are three basic ways to determine rate laws and rate constants/coefficients (Bunnett, 1986; Skopp, 1986; Sparks, 1989, 1995, 1998, 1999): (1) initial rates, (2) directly using integrated equations and graphing the data, and (3) using nonlinear least square analysis.

Let us assume the following elementary reaction between species A, B, and Y,

$$A + B \underset{k_{-1}}{\overset{k_1}{\rightleftharpoons}} Y \qquad [4.4]$$

A forward reaction rate law can be written as

$$d[A]/dt = -k_1[A][B] \qquad [4.5]$$

where k_1 is the forward rate constant and α and β (see Equation [4.2]) are each assumed to be 1.

The reverse reaction rate law for Equation [4.4] is

$$d[A]/dt = +k_{-1}[Y] \qquad [4.6]$$

where k_{-1} is the reverse rate constant.

Equations [4.5] and [4.6] are only applicable far from equilibrium where back or reverse reactions are insignificant. If both forward and reverse reactions are occurring, Equations [4.5] and [4.6] must be combined such that:

$$d[A]/dt = -k_1[A][B] + k_{-1}[Y] \qquad [4.7]$$

Equation [4.7] applies the principle that the net reaction rate is the difference between the sum of all reverse reaction rates and the sum of all forward reaction rates.

One way to ensure that back reactions are not important is to measure initial rates. The initial rate is the limit of the reaction rate as time reaches zero. With an initial rate method, one plots the concentration of a reactant or product over a short reaction time period during which the concentrations of the reactants change so little that the instantaneous rate is hardly affected. Thus, by measuring initial rates, one could assume that only the forward reaction in Equation [4.4] predominates. This would simplify the rate law to that given in Equation [4.5] which as written would be a second order reaction, first order in reactant A and first order in reactant B. Equation [4.5], under these conditions, would represent a second order irreversible elementary reaction. To measure initial rates, one must have available a technique that can measure rapid reactions such as a chemical relaxation method and an accurate analytical detection system to determine product concentrations.

Integrated rate equations can also be used to determine rate constants/coefficients. If one assumes that reactant B in Equation [4.5] is in large excess of reactant A, which is an example of the method of isolation to analyze kinetic data, and $Y_o = 0$, where Y_o is the initial concentration of product Y, Equation [4.5] can be simplified to:

$$d[A]/dt = -k_1'[A] \qquad [4.8]$$

where $k_1' = k_1[B]$

The first order dependence of [A] can be evaluated using the integrated form of Equation [4.8] using the initial conditions at t = 0, $A = A_o$.

$$\log[A]_t = \log[A]_o - \frac{k_1' t}{2.303} \qquad [4.9]$$

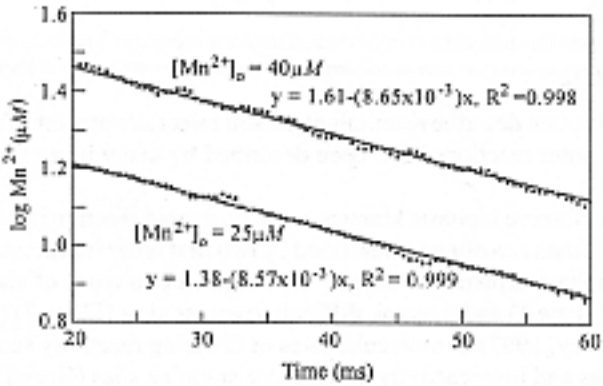

Fig. 4.3 Initial reaction rates depicting the first order dependence of Mn^{2+} sorption as a function of time for initial Mn^{2+} concentrations ($[Mn^{2+}]_o$) 25 and 40 μM [Reprinted from Fendorf et al., 1993. Soil Sci. Soc. Am. J. 57:57-62 with permission of the Soil Science Society of America]

The half-time ($t_{1/2}$) for the above reaction is equal to $0.693/k'_1$ and is the time required for half of reactant A to be consumed.

If a reaction is first order a plot of log $[A]_t$ versus t should result in a straight line with a slope $= k'_1/2.303$ and an intercept of log $[A]_o$. An example of first order plots for Mn^{2+} sorption on δ-MnO_2 at two initial Mn^{2+} concentrations, $[Mn^{2+}]_o$ (25 and 40 μM), is shown in Fig. 4.3. One sees that the plots are linear at both concentrations which would indicate that the sorption process is first order. The $[Mn^{2+}]_o$ values, obtained from the intercepts in Fig. 4.3, were 24 and 41 μM, which are in good agreement with the two $[Mn^{2+}]_o$ values and the rate constants were 3.73×10^{-3} and 3.75×10^{-3} s^{-1}, respectively. The fact that the rate constants do not significantly change with concentration is a good indication that the reaction in Equation [4.8] is first order under the imposed experimental conditions.

It is dangerous to conclude that a particular reaction order is correct, based simply on the conformity of data to an integrated equation. As illustrated above, multiple initial concentrations that vary considerably should be employed to see if the rate is independent of concentration. One should also test multiple integrated equations. It may also be useful to show that reaction rate is not affected by a species whose concentration does not change considerably during an experiment, such as substances not consumed or present in large excess (Bunnett, 1986; Sparks, 1989, 1991, 1995, 1998, 1999).

Least squares analysis can also be used to determine rate constants/coefficients. With this method, one fits the best straight line to a set of points that are linearly related as $y = mx + b$ where y is the ordinate and x is the abscissa datum point, respectively. The slope (m) and the intercept (b) can be calculated by least squares analysis.

When kinetic data are plotted, curvature may be observed due to an incorrect assumption of reaction order. If first-order kinetics is assumed and the reaction is really second order, downward curvature results. If second order kinetics is assumed but the reaction is first order, upward curvature is observed. Curvature can also be due to fractional, third, higher, or mixed reaction order. Nonattainment of equilibrium often results in downward curvature. Temperature changes during the study can also cause curvature; thus, it is important that temperature be accurately controlled during a kinetic experiment.

4.4 Kinetic Models

4.4.1 Ordered Models

First order kinetic models often describe reactions at the soil mineral/water interface. Both single first order and multiple first order reactions have been described by many investigators (Sparks, 1989, 1991; Sparks et al., 1993).

It is not uncommon to observe biphasic kinetics, namely, a rapid reaction rate followed by a much slower reaction rate. Such data can often be described by two first order reactions. Some investigators have interpreted such biphasic kinetics to suggest reactions on two types of sites such as external, readily accessible sites (Slope 1) and internal, difficult to access sites (Slope 2) (Jardine and Sparks, 1984; Comans and Hockley, 1992) or molecular sites of differing reactivity such as high reactivity innersphere complex sites and low reactivity outersphere complex sites (Grossl et al., 1994, 1997).

However, it is unsound to conclude anything about mechanisms based solely on multiple rate constants that are calculated from multiple slopes of kinetic plots. There are other ways to definitively ascertain reaction mechanisms such as calculating energies of activation, elucidating rate limiting steps through stopped flow and interruption approaches, using independent or direct methods to determine mechanisms such as spectroscopic and microscopic techniques, and employing blocking agents that are specific for certain reaction sites. An example of the latter approach is found in the research of Jardine and Sparks (1984) who studied K-Ca exchange on a Delaware soil at three temperatures and observed two apparent simultaneous first order reactions at 283 and 298 K (Fig. 4.4). They hypothesized that the first, more rapid reaction was predominantly due to adsorption on external planar sites of the organic matter and kaolinite in the soil. The slower reaction was ascribed to vermiculitic clay sites that promoted slow pore and surface diffusion. These hypotheses were seemingly validated by using a large organic polymer, cetyltrimethylammonium bromide (CTAB), which because of its size, is sterically hindered from internal sites. Thus, CTAB should only block

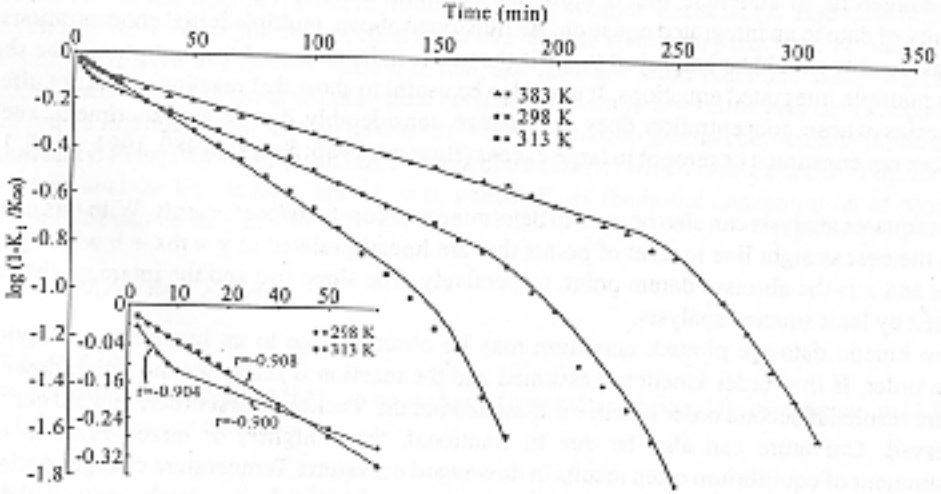

Fig. 4.4 First-order kinetics for potassium adsorption at three temperatures on Evesboro soil with inset showing the initial 50 min of the first-order plots at 298 and 313 K [Reprinted from Jardine and Sparks, 1984. Soil Sci. Soc. Am. J. 48:39-45 with permission of the Soil Science Society of America]

Table 4.1 Linear forms of kinetic equations commonly used in environmental soil chemistry[†]

Zero-order[‡]

$$[A]_t = [A]_o - k_1' t$$

First order

$$\log[A]_t = \log[A]_o - \frac{k_1' t}{2.303^{\S}}$$

Second order[§]

$$\frac{1}{[A]_t} = \frac{1}{[A]_o} + kt$$

Elovich

$$q = (1/\beta)\ln(\alpha\beta) + (1/\beta)\ln t$$

Parabolic Diffusion

$$\left(\frac{1}{t}\right)\left(\frac{Q_t}{Q_\infty}\right) = \frac{4}{\pi^{1/2}}\left(\frac{D}{r^2}\right)^{1/2}\frac{1}{t^{1/2}} - \frac{D}{r^2}$$

Power Function

$$\ln q_t = \ln k + v \ln t$$

[†] From Sparks (1995); terms in equations are defined in the text of the chapter.
[‡] Describing the reaction $A \rightarrow Y$.
[§] $\ln x = 2.303 \log x$, is the conversion from natural logarithms (ln) to base 10 logarithms (log).

external planar sites. When CTAB was applied to the soil, the first slope was eliminated, while the second slope was still present, suggesting multireactive sites.

While first order models have been used widely to describe the kinetics of chemical reactions on natural materials, a number of other simple kinetic models also have been employed. These include various ordered equations such as zero, second, and fractional order, and Elovich, power function or fractional power, and parabolic diffusion models. A brief discussion of some of these will be given; the final forms of the equations are given in Table 4.1. For more complete details and applications of these models, one may consult Sparks (1989, 1995, 1998, 1999).

4.4.2 Elovich Equation

The Elovich equation was originally developed to describe the kinetics of heterogeneous chemisorption of gases on solid surfaces (Low, 1960). It seems to describe a number of reaction mechanisms including bulk and surface diffusion and activation and deactivation of catalytic surfaces.

In soil chemistry, the Elovich equation has been used to describe the kinetics of sorption and desorption of various inorganic materials on soils (Sparks, 1989, 1995, 1998, 1999). It can be expressed as (Chien and Clayton, 1980):

$$q = (1/\beta)\ln(\alpha\beta) + (1/\beta)\ln t \qquad [4.10]$$

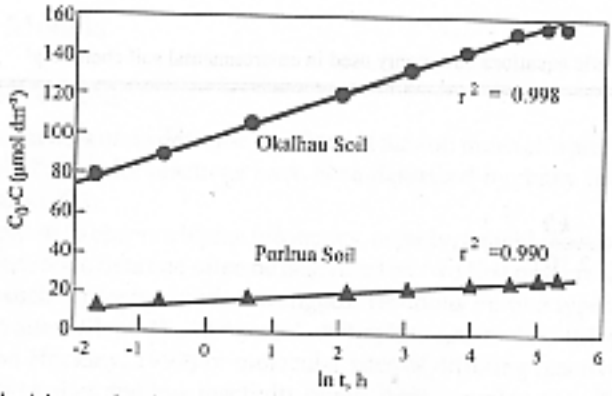

Fig. 4.5 Plot of Elovich equation for phosphate sorption on two soils where C_0 is the initial phosphorus concentration in the soil solution at time t. The quantity $(C_o\text{-}C)$ can be equated to q, the amount sorbed at time t [Reprinted from Chien and Clayton, 1980. Soil Sci. Soc. Am. J. 44:265-268 with permission of the Soil Science Society of America].

where q is the amount of sorbate per unit mass of sorbent at time t and α and ß are constants during any one experiment. A plot of q versus ln t should give a linear relationship if the Elovich equation is applicable with a slope of $(1/\beta)$ and an intercept of $(1/\beta)\ln(\alpha\beta)$. An application of Equation [4.10] to P sorption on soils is shown in Fig. 4.5.

Some investigators have used the α and β parameters from the Elovich equation to estimate reaction rates. For example, it has been suggested that a decrease in β and/or an increase in α would increase reaction rate. However, this is questionable. The slope of plots using Equation [4.10] changes with the concentration of the sorptive and with the solution-to-soil ratio (Sharpley, 1983). Therefore, the slopes are not always characteristic of the soil, but may depend on various experimental conditions.

Some researchers also have suggested that breaks or multiple linear segments in Elovich plots could indicate a changeover from one type of binding site to another (Atkinson et al., 1970). However, such mechanistic suggestions may not be correct (Sparks, 1989, 1995).

4.4.3 Parabolic Diffusion Equation

The parabolic diffusion equation is often used to suggest that diffusion-controlled phenomena are rate limiting. It was originally derived from radial diffusion in a cylinder where the ion concentration on the surface is constant, and initially, the ion concentration within the cylinder is uniform. It is also assumed that ion diffusion through the upper and lower faces of the cylinder is negligible. Following Crank (1976), the parabolic diffusion equation, as applied to soils can be expressed as

$$(Q_t / Q_\infty) = \frac{4}{\pi^{1/2}}\left(\frac{Dt}{r^2}\right)^{1/2} - \frac{Dt}{r^2} - \frac{1}{3\pi^{1/2}}\left(\frac{Dt}{r^2}\right)^{3/2} \qquad [4.11]$$

where r is the radius of the cylinder, Q_t is the quantity of diffusing substance that has left the cylinder at time t, Q is the corresponding quantity after infinite time, and D is an apparent diffusion coefficient.

For the relatively short times in most experiments, the third and subsequent terms may be ignored, and thus

$$\frac{Q_t}{Q_\infty} = \frac{4}{\pi^{1/2}}\left(\frac{Dt}{r^2}\right)^{1/2} - \frac{Dt}{r^2}$$

or [4.12]

$$\frac{1}{t}\left(\frac{Q_t}{Q_\infty}\right) = \frac{4}{\pi^{1/2}}\left(\frac{D}{r^2}\right)^{1/2}\frac{1}{t^{1/2}} - \frac{D}{r^2}$$

and thus, a plot of $\frac{Q_t / Q_\infty}{t}$ versus $1/t^{1/2}$ should give a straight line with a slope of

$$\frac{4}{\pi^{1/2}}\left(\frac{D}{r^2}\right)^{1/2}$$

and intercept $(-D/r^2)$. Thus, if r is known, D may be calculated from both the slope and intercept.

The parabolic diffusion equation has successfully described metal reactions on soils and soil constituents (Chute and Quirk, 1967; Jardine and Sparks, 1984; Krishnamurti and Huang, 1992; Krishnamurti et al., 1997), feldspar weathering (Wollast, 1967), and pesticide reactions (Weber and Gould, 1966).

4.4.4 Fractional Power or Power Function Equation

This equation can be expressed as

$$q = kt^v \qquad [4.13]$$

where q is amount of sorbate per unit mass of sorbent at time t, k and v are constants and v is positive and < 1. Equation [4.13] is empirical, except for the case where $v = 0.5$, when it is similar to the parabolic diffusion equation.

Equation [4.13] and various modified forms have been used by a number of researchers to describe the kinetics of reactions in natural materials (Kuo and Lotse, 1974; Havlin and Westfall, 1985).

4.4.5 Z(t) and Diffusion Models

In a number of studies, several simple kinetic models have described rate data well, based on correlation coefficients and standard errors of the estimate (Chien and Clayton, 1980; Onken and Matheson, 1982; Sparks and Jardine, 1984; Allen et al, 1995). Despite this, there is often an inconsistent relation between the equation that gives the best fit and the physicochemical and mineralogical properties of the sorbent(s) being studied. Another problem with some of the kinetic models is that they are empirical and no meaningful rate parameters can be obtained.

Aharoni and Ungarish (1976) and Aharoni (1984) noted that some simple kinetic models are approximations of more general expressions within certain limited time ranges. They suggested a generalized empirical equation by examining the applicability of power function, Elovich, and first order equations to experimental data. By writing these as the explicit functions of the reciprocal of the rate (Z) which is $(dq/dt)^{-1}$, one can show that a plot of Z versus t should be convex if the power function

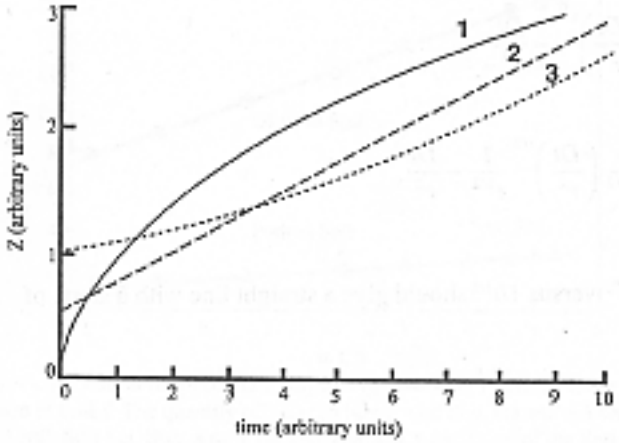

Fig. 4.6 Plot of Z vs. time implied by (1) power function model, (2) Elovich model, and (3) first order model. The equations for the models were differentiated and expressed as explicit functions of the reciprocal of the rate, Z [Reprinted from Aharoni and Sparks, 1991. Soil Sci. Soc. Am. Spec Pub. 27 with permission of the Soil Science Society of America].

equation is operational (1 in Fig. 4.6); linear, if the Elovich equation is appropriate (2 in Fig. 4.6); and concave, if the first order equation is appropriate (3 in Fig. 4.6). However, such plots for soil systems (Fig. 4.7) are usually S shaped, convex at small, concave at large, and linear at some intermediate t value suggesting that the reaction rate can best be described by the power function, first order and Elovich equations in these ranges of t, respectively. Thus, the S-shaped curve indicates that the above equations may be applicable, each over some limited time range.

One of the reasons a particular kinetic model appears to be applicable may be that the study is conducted during the time range when the model is most appropriate. While sorption, for example, decreases over many orders of magnitude before equilibrium is approached, with most methods and

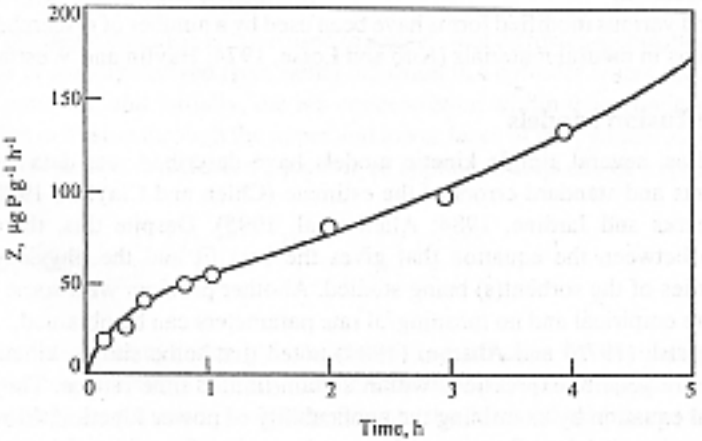

Fig. 4.7 Sorption of phosphate by a Typic Dystrochrept soil plotted as Z vs. time. The circles represent the experimental data of Polyzopoulos et al. (1986). The solid line is a curve calculated according to a homogeneous diffusion model [Reprinted from Aharoni and Sparks, 1991. Soil Sci. Soc. Am. Spec Pub. 27 with permission of the Soil Science Society of America].

experiments, only a portion of the entire reaction is measured, and over this time range, the assumptions associated with a simple kinetic model (power function, Elovich, and first order) are valid. Aharoni and Suzin (1982a,b) showed that the S-shaped curves could be well described using homogeneous and heterogeneous diffusion models. In homogeneous diffusion situations, the final and initial portions of the S-shaped curves (conforming to the power function and first order equations, respectively) predominated, whereas in instances where the heterogeneous diffusion model was operational, the linear portion of the S-shaped curve that conformed to the Elovich equation predominated. Derivations of homogeneous and heterogeneous diffusion models can be found in Aharoni and Sparks (1991).

4.4.6 Implications of Diffusion Models

The finding that slower reactions at the soil mineral/liquid interface can be described by diffusional models indicates that the kinetics of chemical processes cannot be considered separately from physically limited transport phenomena. Thus, such a combination of processes cannot be treated using first or other order chemical kinetics equations. When one states that a reaction between the molecular species A and B is first order with respect to A, one assumes that the molecules of A have equal chances of participating in the reaction, and therefore, the rate is proportional to the concentration (C_A). This reasoning can be extended to a reaction between a sorbing surface and a sorptive. In this case, C_A refers to the number of reactive sites per unit area, which corresponds to the number of unoccupied sites per unit area ($1-\theta_A$). However, by using first order kinetics (or other order kinetics), one tacitly assumes that all the surface sites are potential reactants at any time, and have an opportunity of participating in the sorption process. If one assumes that there are sites that cannot be reached directly from the fluid phase, but can be reached after the sorbate has undergone sorption and desorption at other sites, one cannot separate chemical kinetics from diffusion limited kinetics. The overall kinetic process obeys a diffusion equation since diffusion is the rate limiting process. However, the diffusion coefficient, which reflects the rate at which the sorbate jumps from one site to another, is determined by the rate of the chemical reactions by which the sorbent-sorbate bonds are created and destroyed. Additionally, the activation energy for diffusion is equivalent to the activation energy of the chemical reaction.

4.4.7 Multiple Site Models

Based on the previous discussion, it is evident that simple chemical kinetics models such as ordered reaction, power function and Elovich models may not be appropriate to describe reactions in heterogeneous systems such as soils, sediments, and soil components. In these systems where there is a range of particle sizes and multiple retention sites, both chemical kinetics and transport phenomena are occurring simultaneously, and a fast reaction is often followed by a slower reaction(s). In such systems, nonequilibrium models that describe both chemical and physical nonequilibrium and that consider multiple components and sites are more appropriate. Physical nonequilibrium is ascribed to some rate limiting transport mechanism such as FD or PD, while chemical nonequilibrium is due to a rate limiting mechanism at the particle surface (CR). Nonequilibrium models include two-site, multiple site, radial diffusion (pore diffusion), surface diffusion, and multiprocess models (Table 4.2). Emphasis here will be placed on the use of these models to describe sorption phenomena.

The term sites can have a number of meanings (Brusseau and Rao, 1989): (1) specific, molecular scale reaction sites; (2) sites of differing degrees of accessibility (external, internal); (3) sites of differing sorbent type (organic matter and inorganic mineral surfaces); and (4) sites with different sorption mechanisms. With chemical nonequilibrium sorption processes, the sorbate may undergo two

or more types of sorption reactions, one of which is rate limiting. For example, a metal cation may sorb to organic matter by one mechanism and to mineral surfaces by another mechanism, with one of the mechanisms being time dependent.

4.4.7.1 Chemical Nonequilibrium Models

Chemical nonequilibrium models describe time-dependent reactions at sorbent surfaces. The one-site model is a first order approach that assumes that the reaction rate is limited by only one process or mechanism on a single class of sorbing sites and that all sites are of the time-dependent type. In many cases, this model appears to describe soil chemical reactions quite well. However, often it does not. This model would seem not appropriate for most heterogeneous systems since multiple sorption sites exist.

The two-site (two compartment, two box) or bicontinuum model has been widely used to describe chemical nonequilibrium (Leenheer and Ahlrichs, 1971; Hamaker and Thompson, 1972; Karickhoff, 1980; McCall and Agin, 1985; Karickhoff and Morris, 1985; Jardine et al., 1992) and physical nonequilibrium (Nkedi-Kizza et al., 1984; Lee et al., 1988; van Genuchten and Wagenet, 1989) (Table 4.2). This model assumes that there are two reactions occurring, one that is fast and reaches equilibrium quickly and a slower reaction that can continue for long time periods. The reactions can occur either in series or in parallel (Brusseau and Rao, 1989).

In describing chemical nonequilibrium with the two-site model, two types of sorbent sites are assumed. One site involves an instantaneous equilibrium reaction and the other, the time-dependent reaction. The former is described by an equilibrium isotherm equation while a first order equation is usually employed for the latter.

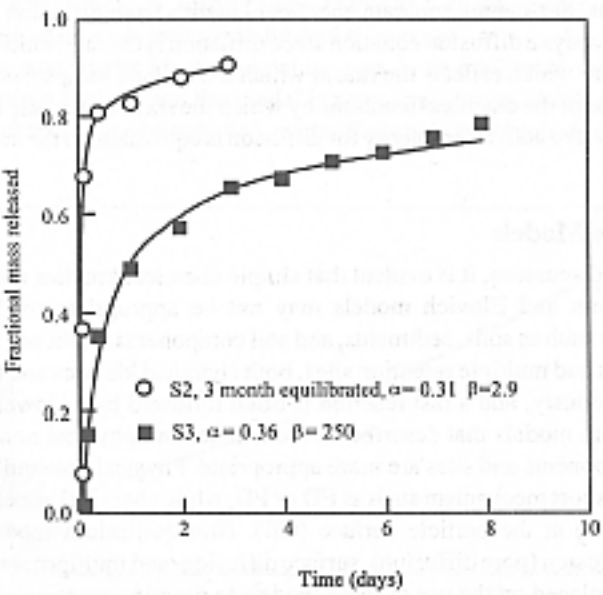

Fig. 4.8 Mass fractional release of naphthalene from two soils, S2 and S3 (S2 is a freshly contaminated soil, reacted with naphthalene for 3 months and S3 is a field [aged] contaminated soil) fitted with a multisite continuum compartment (Γ) model [Reprinted with permission from Connaughton et al., 1993. Environ. Sci. Technol. 27:2397-2403. Copyright American Chemical Society]

With the two-site model, there are two adjustable or fitting parameters, the fraction of sites at local equilibrium (X_1) and the rate constant (k). A distribution (K_d) or partition coefficient (K_p) is determined independently from a sorption/desorption isotherm.

To account for the multiple sites that may exist in heterogeneous systems, Connaughton et al. (1993) developed a multisite compartment (continuum) model (Γ) that incorporates a continuum of sites or compartments with a distribution of rate coefficients that can be described by a gamma density function. A fraction of the sorbed mass in each compartment is at equilibrium with a desorption rate coefficient or distribution coefficient for each compartment or site (Table 4.2). The multisite model has two fitting parameters α, a shape parameter, and $1/\beta$, which is a scale parameter that determines the mean standard deviation of the rate coefficients. Fig. (4.8) shows application of the Γ model to desorption of naphthalene from contaminated soils. The entire desorption process was described well with this model.

4.4.7.2 Physical Nonequilibrium Models

A number of models can be used to describe physical nonequilibrium reactions. Since transport processes in the mobile phase are not usually rate limiting, physical nonequilibrium models focus on diffusion in the immobile phase or interaggregate/diffusion processes such as pore and/or surface diffusion. The transport between mobile and immobile regions is accounted for in physical nonequilibrium models in three ways (Brusseau and Rao, 1989): (1) explicitly with Fick's law to describe the physical mechanism of diffusive transfer, (2) explicitly by using an empirical first order mass transfer expression to approximate solute transfer, and (3) implicitly by using an effective or lumped dispersion coefficient that includes the effects of sink/source differences and hydrodynamic dispersion and axial diffusion.

A pore diffusion model (Table 4.2) has been used by a number of investigators to study sorption processes using batch systems (Wu and Gschwend, 1986; Steinberg et al., 1987; Ball and Roberts, 1991; Harmon et al., 1992; Pignatello et al., 1993). Wu and Gschwend (1986) successfully used the pore diffusion model to describe chlorobenzene congener sorption/desorption on soils and sediments. Fig. 4.9 shows experimental and model fits for tetrachlorobenzene and pentachlorobenzene sorption on soils. The sole fitting parameter in this model is the effective diffusion coefficient (D_e) which may be estimated *a priori* from chemical and colloidal properties. However, this estimation is only valid if the sorbent material has a narrow particle size distribution so that an accurate, average particle size can be defined. Moreover, in the pore diffusion model, an average representative D_e is assumed, which means there is a continuum in properties across an entire pore size spectrum. This is not a valid assumption for micropores in which there are higher adsorption energies of sorbates causing increased sorption. The increased sorption reduces diffusive transport rates and results in nonlinear isotherms for sorbents with pores less than several sorbate diameters in size. Other factors can cause reduced transport rates in micropores including steric hindrance, which increases as the pore size approaches the solute size and greatly increased surface area to pore volume ratios (which occurs as pore size decreases).

Another problem with the pore diffusion model is that sorption and desorption kinetics may have been measured over a narrow concentration range. This is a problem since a sorption/desorption mechanism in micropores at one concentration may be insignificant at another concentration.

Fuller et al. (1993) used a pore space diffusion model (Table 4.2) to describe arsenate adsorption on ferrihydrite that included a subset of sites whereby sorption was at equilibrium. A Freundlich model was used to describe sorption on these sites. Diffusion into the particle was described by Fick's second

Table 4.2 Comparison of sorption kinetic models[1,2]

Conceptual model	Fitting parameter(s)	Model limitations
one-site model k_d $S \rightleftharpoons C$	k_d	cannot describe biphasic sorption/desorption
two-site model $X_1 K_p k_d$ $S_1 \rightleftharpoons C \rightleftharpoons S_2$	k_d, K_p[1], X_1	may not describe the "bleeding" or slow, reversible, nonequilibrium desorption for residual sorbed compounds (Karickhoff, 1980)
radial diffusion penetration retardation (pore diffusion) model (Wu and Gschwend, 1986) K_p, D_{eff} $S \rightleftharpoons C' \rightleftharpoons C$	D_{eff}[1] = f(n,t)$D_w n/(1-n)\rho_s K_p$	cannot describe instantaneous uptake without additional correction factor; did not describe kinetic data for times greater than 10^3 min (Wu and Gschwend, 1986)
dual-resistance surface diffusion model (Miller and Pedit, 1992) D_s, k_b $S' \rightleftharpoons C'_s \rightleftharpoons C$	D_s, k_b	model calibrated with sorption data predicted more desorption than occurred in the desorption experiments (Miller and Pedit, 1992)
multisite continuum compartment model (Connaughton et al., 1993) $F(t) = 1 - \frac{M(t)}{M} = 1 - \left(\frac{\beta}{\beta + t}\right)^{\alpha}$	α, β	assumption of homogeneous, spherical particles and diffusion only in aqueous phase
pore space diffusion model (Fuller et al., 1993) $\left(\epsilon + \frac{S_w}{n} K_s C(r)^{(1-1/n)}\right) \frac{\partial C(r)}{\partial t} =$ $D_e \left(\frac{\partial^2 C(r)}{\partial r^2} + \frac{2\partial C(r)}{r\partial r}\right)$	D_e, ϵ, K_s, 1/n, F_{eq}	
multiple particle class pore diffusion model (Pedit and Miller, 1995) $\left(\frac{\theta'_p + \rho'_a}{\partial C'_p}\right) \frac{\partial q'_r(r,t)}{(r,t)} \frac{\partial C'_p(r,t)}{\partial t} =$ $\frac{\theta'_p D'_p}{r^2} \frac{\partial}{\partial r}\left(\frac{r^2 \partial C'_p(r,t)}{\partial r}\right)$ $-\theta'_p \lambda'_p C'_p(r,t) - \rho'_a \lambda'_r q'_r(r,t)$	θ'_p, ρ'_a, D'_p, λ'_p, λ'_r	multiple fitting parameters; variations in sorption equilibrium and rates that might occur within a particle class or an individual particle grain are not addressed.

[1] Partially adapted from Connaughton et al. (1993).

[2] Abbreviations used are as follows: S, concentration of the bulk sorbed contaminant (g g^{-1}); C, concentration of the bulk aqueous-phase contaminant (g mL^{-1}); k_d, first-order desorption rate coefficient (min^{-1}); S_1, concentration of the sorbed contaminant that is rate limited (g g^{-1}); S_2, concentration of the contaminant that is in equilibrium with the bulk aqueous concentration (g g^{-1}); X_1, fraction of the bulk sorbed contaminant that is in equilibrium with the aqueous concentration; K_p, sorption equilibrium partition coefficient (mL g^{-1}); D_{eff}, effective diffusivity of sorbate molecules or ions in the particles (cm^2 s^{-1}); S', concentration of contaminant in immobile bound state (mol g^{-1}); C', concentration of contaminant free in the pore fluid (mol cm^{-3}); n, porosity of the sorbent (cm^3 of fluid cm^{-3}); D_w, pore fluid diffusivity of the sorbate (cm^2 s^{-1}); ρ_s, specific gravity of the sorbent (g cm^{-3}); f (n,t), pore geometry factor; k_b, boundary layer mass transfer coefficient (m s^{-1}); r, radius of the spherical solid particle, assumed constant (m); ρ, macroscopic particle density of the solid phase (g m^{-3}); C'_s, solution-phase solute concentration corresponding to an equilibrium with the solid-phase solute concentration at the exterior of the particle (g L^{-1}); D_s, surface diffusion coefficient (m s^{-1}). § K_p can be determined independently. [1] K_p, D_w, and ρ_s can be determined independently; F(t), fraction of mass released through time t; M(t), mass remaining after time t; M, total initial mass; β, scale parameter necessary for determination of mean and standard deviation of k_s; α, shape parameter; ϵ, internal porosity of sorbent; C(r), concentration of sorptive in the aqueous phase in the pore fluid at radial distance r; S_w is the surface of sorbent per unit volume of solid; 1/n, the adsorption isotherm slope; K_s, adsorption isotherm intercept; D_e, effective diffusion coefficient; a, radius of the aggregate; F_{eq}, equilibrium fraction of adsorption sites; θ'_p, intraparticle porosity of particle class I; ρ'_a, apparent particle density of particle class I; r, radial distance; C'_p (r, t), intraparticle fluid-phase solute concentration of the particle class I; D'_p, pure diffusion coefficient for particle class I; λ'_p, intraparticle fluid-phase first-order reaction rate coefficient for particle class I; λ'_r, intraparticle solid-phase first-order reaction rate coefficient for particle class I, q'_r (r, t), intraparticle solid-phase solute concentration of particle class I.

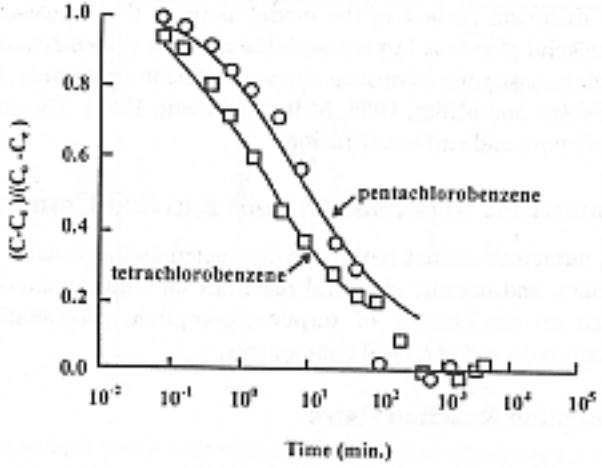

Fig. 4.9 Experimental and model fitting results for pentachlorobenzene and tetrachlorobenzene sorption on Iowa soils where C is the dissolved concentration of organic chemical in the bulk solution, C_o is the initial concentration and C_e is the equilibrium concentration. The points represent experimental data and the solid lines represent fit of the data to the radial diffusion (pore diffusion) model [Reprinted with permission from Wu and Gschwend, 1986. Environ. Sci. Technol. 20:717-725. Copyright American Chemical Society].

law of diffusion; homogeneous, spherical aggregates, and diffusion only in the aqueous phase were assumed. Fig. 4.10 shows the fit of the model when sorption at all sites was controlled by intra-aggregate diffusion. The fit was better when sites that had attained sorption equilibrium were included based on the assumption that there was an initial rapid sorption on external surface sites before intra-aggregate diffusion.

Pedit and Miller (1995) have developed a general multiple particle class pore diffusion model that accounts for differences in physical and sorptive properties for each particle class (Table 4.2). The model includes both instantaneous equilibrium sorption and time-dependent pore diffusion for each

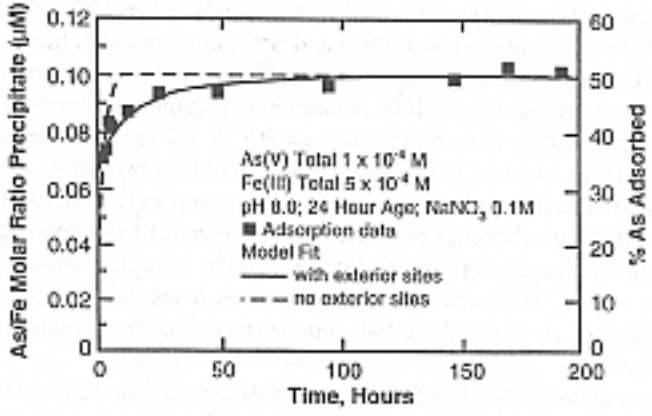

Fig. 4.10 Comparison of pore space diffusion model fits of As (V) sorption with experimental data (dashed curve represents sorption where all surface sites are diffusion limited and the solid curve represents sorption on equilibrium sites plus diffusion limited sites) [Reprinted from Fuller et al., 1993. Surface chemistry of ferrihydrite. 2. Geochim. Cosmochim. Acta 57:2271-2282, with kind permission of Elsevier Science, Amsterdam, Netherlands]

particle class. The pore diffusion portion of the model assumes that solute transfer between the intraparticle fluid and the solid phases is fast *vis-à-vis* interparticle pore diffusion processes.

Surface diffusion models, assuming a constant surface diffusion coefficient, have been used by a number of researchers (Weber and Miller, 1988; Miller and Pedit, 1992). The dual resistance model (Table 4.2) combines both pore and surface diffusion.

4.5 Kinetics of Important Reactions on Soils and Soil Components

In the past two decades, numerous studies have been conducted on the kinetics of metal, oxyanion, radionuclide, plant nutrient, and organic chemical reactions on natural materials. In this section, emphasis will be placed on the kinetics of sorption/desorption, precipitation/dissolution, and oxidation/reduction reactions on soils and soil components.

4.5.1 Sorption/Desorption Reaction Rates

4.5.1.1 Heavy Metals and Oxyanions

Chemical reactions of heavy metals on soil components are rapid, occurring on a millisecond time scale. For such rapid reactions, chemical techniques such as pressure jump (p-jump) relaxation must be employed (Hayes and Leckie, 1986; Sparks, 1989; Sparks and Zhang, 1991; Grossl and Sparks, 1995; Sparks et al., 1996).

The use of p-jump relaxation to measure the kinetics of ion sorption/desorption on metal oxide surfaces was pioneered by several Japanese chemists. Their research includes some of the following sorption/desorption kinetic studies: divalent metal ion (Hachiya et al., 1984), phosphate (Mikami et al., 1983a), chromate (Mikami et al., 1983b), and uranyl (Mikami et al., 1983c) sorption reactions on γ-Al_2O_3. Hayes and Leckie (1986) were the first to use p-jump relaxation to study sorption/desorption kinetics of a metal ion contaminant (Pb^{2+}) on goethite (α-FeOOH). Other successive studies monitored the rapid sorption/desorption kinetics of molybdate (Zhang and Sparks, 1989), sulfate (Zhang and Sparks, 1990a), selenate and selenite (Zhang and Sparks, 1990b), Cu^{2+} (Grossl et al., 1994), and arsenate and chromate (Grossl et al., 1997) on goethite. Additional studies have investigated borate sorption/desorption kinetics on pyrophyllite (Keren et al., 1994) and on γ-Al_2O_3 (Toner and Sparks, 1995).

Details of many of these studies are summarized in Hayes and Leckie (1986), Sparks (1989, 1995), Sparks and Zhang (1991) and Sparks et al. (1996) and will not be detailed here. A recent study of Grossl et al. (1997) will be summarized to illustrate rapid CR rates of two environmentally important oxyanions (chromate and arsenate) on goethite. A double relaxation was observed for both arsenate and chromate sorption/desorption over a pH range of 6.5 to 7.5 for arsenate and 5.5 to 6.5 for chromate, respectively (Figs. 4.11–4.12). Based on the double relaxations, a two-step process, resulting in the formation of an innersphere bidentate surface complex (Fig. 4.13) was proposed. The first step involves an initial ligand exchange reaction of the aqueous oxyanion (H_2AsO^- or $HCrO_4^-$) with goethite, forming an innersphere monodentate surface complex which produces signals associated with fast τ values. The succeeding step involves a second ligand exchange reaction, resulting in the formation of an innersphere bidentate surface complex which produces the signal associated with slow τ values.

To determine if the mechanism displayed in Fig. 4.13 was plausible and consistent with the kinetic data, the following linearized rate equations relating reciprocal relaxation time values (τ^{-1}) to the concentrations of reactive species were used:

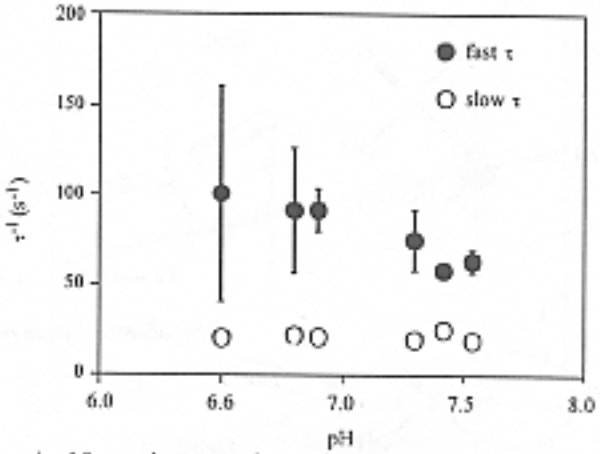

Fig. 4.11 τ^{-1} values determined from p-jump experiments for arsenate adsorption/desorption on goethite, as a function of pH [Reprinted with permission from Grossl et al. (1997). Environ. Sci. Technol. 31:321-326. Copyright American Chemical Society]

$$\tau^{-1}_{fast} + \tau^{-1}_{slow} = k_1 \quad \left([XOH] + [ion\ species]\right) + k_{-1} + k_2 + k_{-2} \qquad [4.14]$$

$$\tau^{-1}_{fast} \cdot \tau^{-1}_{slow} = k_1\left[k_2 + k_{-2}\right] \quad \left([XOH] + [ion\ species]\right) + k_{-1}k_{-2} \qquad [4.15]$$

where the ion species are $H_2AsO_4^-$ or $HCrO_4^-$. The derivation of these equations was obtained from Bernasconi (1976) and is based on the two-step reaction system ($A + B \leftrightarrow C \leftrightarrow D$). If the mechanism portrayed in Fig. 4.13 is accurate, then a plot of $\tau^1_{fast} + \tau^{-1}_{slow}$ and $\tau^1_{fast} \cdot \tau^{-1}_{slow}$ as a function of the concentration term ($[XOH] + [ion\ species]$) should be linear. Plots of Equations [4.14] and [4.15] were linear for both arsenate and chromate suggesting that the proposed mechanism was plausible (Figs. 4.14–4.15).

From the plots in Figs. 4.14–4.15, forward and reverse rate constants were obtained for the sorption and desorption reactions of both the monodentate and bidentate steps; where k_1 = slope (Fig. 4.14);

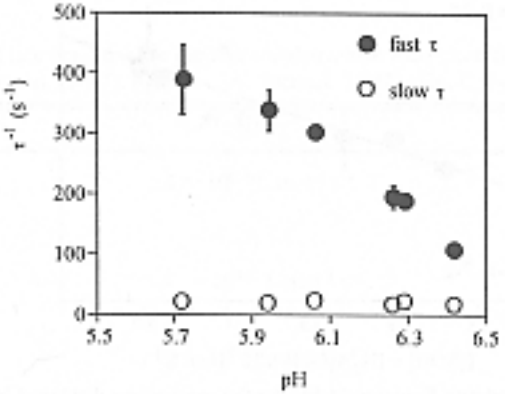

Fig. 4.12 τ^{-1} values determined from p-jump experiments for chromate adsorption/desorption on goethite, as a function of pH [Reprinted with permission from Grossl et al. (1997). Environ. Sci. Technol. 31:321-326. Copyright American Chemical Society]

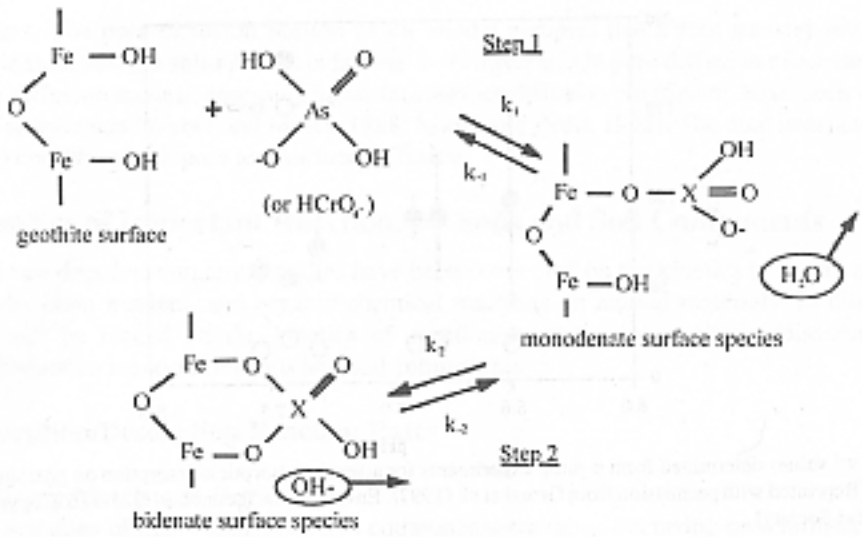

Fig. 4.13 Proposed mechanism for oxyanion adsorption/desorption on goethite. The X represents either As(V) or Cr(VI) [Reprinted with permission from Grossl et al., 1997. Environ. Sci. Technol. 31:321-326. Copyright American Chemical Society].

k_{-1} = intercept (Fig. 4.14) – slope (Fig. 4.15)/slope (Fig. 4.14); k_2 = intercept (Fig. 4.14) – k_{-1} – k_{-2}; and k_{-2} = intercept (Fig. 4.15)/k_{-1}. The calculated rate constants for both chromate and arsenate adsorption/desorption on goethite are listed in Table 4.3.

Overall, the forward rate constants associated with the formation of the innersphere oxyanion/goethite surface complexes were more rapid than the reverse rate constants. Therefore, the rate limiting steps were the reverse reactions. The equilibrium constants listed in Table 4.3 were calculated

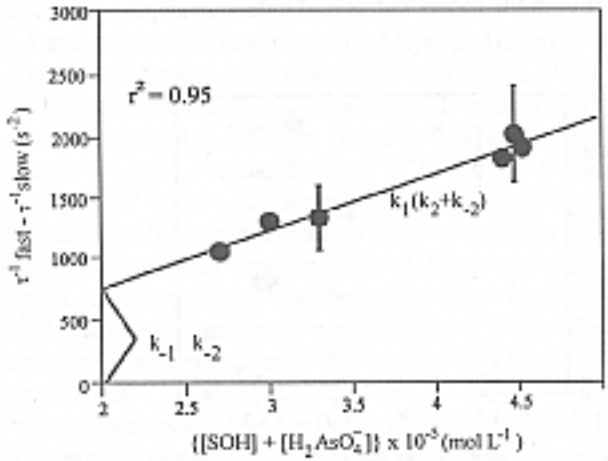

Fig. 4.14 Evaluation of the linearized rate Equation [4.14] for the mechanism displayed in Fig. 4.13 for arsenate [Reprinted with permission from Grossl et al. (1997). Environ. Sci. Technol. 31:321-326. Copyright American Chemical Society]

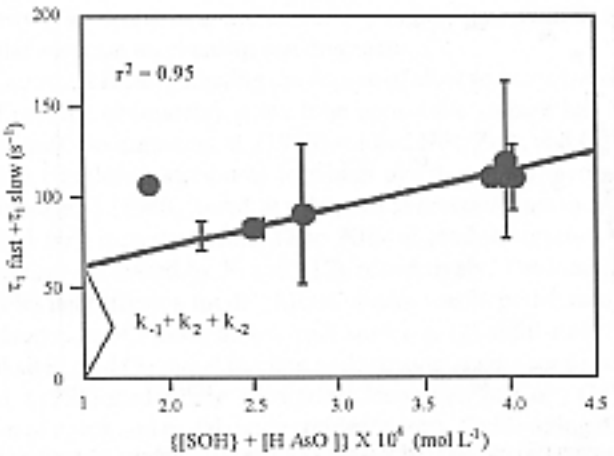

Fig. 4.15 Evaluation of the linearized rate Equation [4.15] for the mechanism displayed in Fig. 4.13 for arsenate [Reprinted with permission from Grossl et al. (1997). Environ. Sci. Technol. 31:321-326. Copyright American Chemical Society]

using the rate constants for each reaction step in the proposed mechanism (Fig. 4.13) from the following relationship:

$$K_{eq} = k_1 / k_{-1} \qquad [4.16]$$

The calculated equilibrium constant for step 1 for arsenate was $10^{4.35}$ and for step 2 was $10^{0.26}$, while the calculated K_{eq} for step 1 for chromate was $10^{5.7}$ and for step 2 was $10^{-0.4}$. The sorption of both oxyanions and subsequent formation of innersphere surface complexes are thermodynamically favorable, with the exception of the equilibrium constant for the second step associated with chromate sorption (slightly less than 1). Thus, the monodentate chromate/goethite surface complex is slightly favored over the bidendate surface complex. This is in agreement with spectroscopic data obtained from X-ray absorption fine structure (XAFS) analyses (Fendorf et al., 1997) which indicate a mixture of both monodentate and bidentate arsenate, and chromate surface complexes; but at low surface coverage, a greater proportion of chromate is associated with the monodentate complex than the

Table 4.3 Calculated rate constants for chromate and arsenate adsorption/desorption on goethite [Reprinted with permission from Grossl et al. (1997). Environ. Sci. Technol. 31:321-326. Copyright American Chemical Society]

	Step I	Step II
Arsenate	$k_1 = 10^{5.3}$ L mol^{-1} s^{-1}	$k_2 = 15$ s^{-1}
	$k_{-1} = 8$ s^{-1}	$k_{-2} = 8$ s^{-1}
	$K_{eq} = 10^{4.35}$ L mol^{-1} s^{-1}	$K_{eq} = 10^{0.26}$
Chromate	$k_1 = 10^{5.8}$ L mol^{-1} s^{-1}	$k_2 = 16$ s^{-1}
	$k_{-1} = 129$ s^{-1}	$k_{-2} = 38$ s^{-1}
	$K_{eq} = 10^{5.7}$ L mol^{-1} s^{-1}	$K_{eq} = 10^{-0.4}$

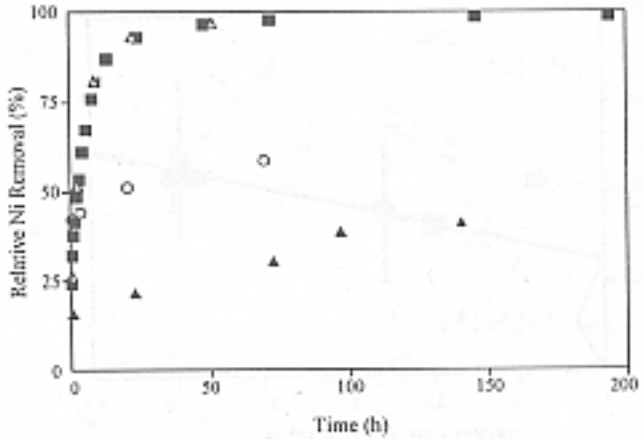

Fig. 4.16 Kinetics of Ni sorption [%] on pyrophyllite (■), kaolinite (△), gibbsite (▲) and montmorillonite (o) from a 3 m*M* Ni solution at pH = 7.5 and an ionic strength I = 0.1*M* ($NaNO_3$). The last sample of each experiment was collected and analyzed by XAFS [Reprinted from Scheidegger et al.,1997. J. Colloid Interf. Sci. 186:118-128. with permission]

bidentate complex. The results from both kinetic and XAFS experiments suggest that arsenate is more likely to form an innersphere surface complex with goethite than chromate.

While the initial sorption of heavy metals is rapid, with the CR step occurring on millisecond time scales, further sorption is usually quite slow (Fig. 4.16) occurring over time scales of days and longer. This slow sorption has been ascribed to several mechanisms including interparticle or intraparticle diffusion in pores and solids, sites of low reactivity, and surface precipitation/nucleation (Sparks, 1998; Strawn and Sparks, 1997, unpublished data). With heterogeneous soils and even soil components, there may be a continuum between the three sorption mechanisms, for example, between adsorption and surface precipitation/nucleation. While it has generally been assumed that adsorption in comparison to surface precipitation/nucleation is much more rapid, recent studies (Scheidegger et al., 1998) that will be discussed later, have shown that surface precipitation/nucleation processes can occur on time scales as short as 15 min which indicates that sorption and nucleation processes can

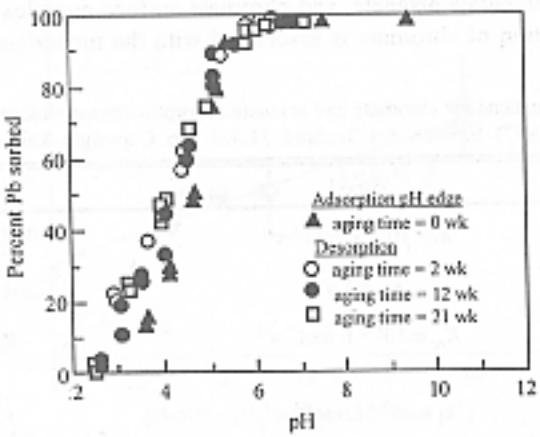

Fig. 4.17 Fractional sorption-desorption of Pb^{2+} to hydrousFe(III) as a function of pH and HFO-Pb^{2+} aging time [reprinted from Ainsworth et al., 1994. Soil Sci. Soc. Am. J. 58:1615-1623 with permission of the Soil Science Society of America]

occur simultaneously. However, in some cases, depending on reaction conditions and the metal involved, a particular sorption mechanism can dominate.

Obviously, an important factor affecting the degree of slow sorption/desorption of metals (and for that matter also of organic chemicals) is the time period the sorbate has been in contact with the sorbent (residence time). Bruemmer et al. (1988) studied Ni^{2+}, Zn^{2+}, and Cd^{2+} sorption on goethite, a porous Fe oxide that has defect structures in which metals can be incorporated to satisfy charge imbalances. Bruemmer et al. (1988) found, at pH 6, that as reaction time increased from 2 hr to 42 days (at 293 K), adsorbed Ni^{2+} increased from 12 to 70% of total adsorption, and total Zn^{2+} and Cd^{2+} adsorption over this time increased by 33 and 21%, respectively. The kinetic reactions could be well described using a Fickian diffusion model. Metal uptake was hypothesized to occur by a three-step mechanism: (1) adsorption of metals on external surfaces, (2) solid-state diffusion of metals from external to internal sites, and (3) metal binding and fixation at positions inside the goethite particle.

Ainsworth et al. (1994) studied the adsorption/desorption of Co^{2+}, Cd^{2+}, and Pb^{2+} on hydrous Fe(III) as a function of aging and metal oxide residence time. Oxide aging did not cause hysteresis of metal cation sorption/desorption. Aging the oxide with the metal cations resulted in hysteresis with Cd^{2+} and Co^{2+} but little with Pb^{2+}. With Pb^{2+} between pH 3 and 5.5 there was slight hysteresis over a 21-week aging process (hysteresis varied from < 2% difference between sorption and desorption to ~10%). At pH 2.5, Pb^{2+} desorption was complete within a 16-h period and was not affected by aging time (Fig. 4.17). However, with Cd^{2+} and Co^{2+}, extensive hysteresis was observed over a 16-week aging period and the hysteresis increased with aging time (Figs. 4.18–4.19). After 16 weeks of aging, 20% of the Cd^{2+} and 53% of the Co^{2+} was not desorbed, and even at pH 2.5, hysteresis was observed. The extent of reversibility with aging for Co^{2+}, Cd^{2+}, and Pb^{2+} was inversely proportional to the ionic radius of the ions, namely, $Co^{2+} < Cd^{2+} < Pb^{2+}$. Ainsworth et al. (1994) attributed the hysteresis to Co and Cd incorporation into a recrystallizing solid (probably goethite) by isomorphic substitution and not to micropore diffusion.

Fuller et al. (1993) combined kinetic sorption and desorption experiments with spectroscopic observations (Waychunas et al., 1993) to study As sorption on ferrihydrite. Using XAFS spectroscopy, they found that As was sorbed predominantly as innersphere bidentate complexes, regardless of whether the As was adsorbed after the mineralization of the ferrihydrite, or it was present during precipitation. No As surface precipitates were observed. Slow As sorption and desorption were

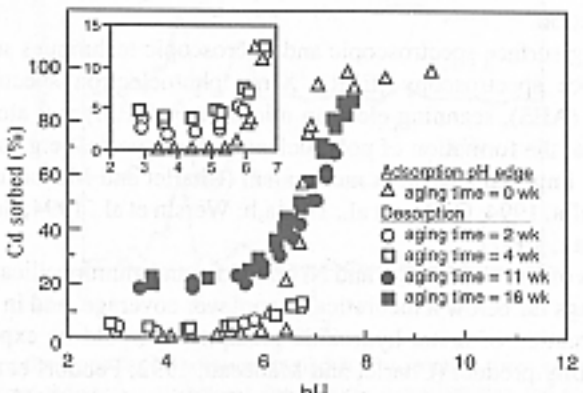

Fig. 4.18 Fractional sorption-desorption of Cd^{2+} to hydrous Fe-oxide (HFO) as a function of pH and HFO-Cd^{2+} aging time; insert shows adsorption-desorption of Cd^{2+} to HFO at 2- and 4-wk aging times [Reprinted from Ainsworth et al., 1994. Soil Sci. Soc. Am. J. 58:1615-1623 with permission of the Soil Science Society of America]

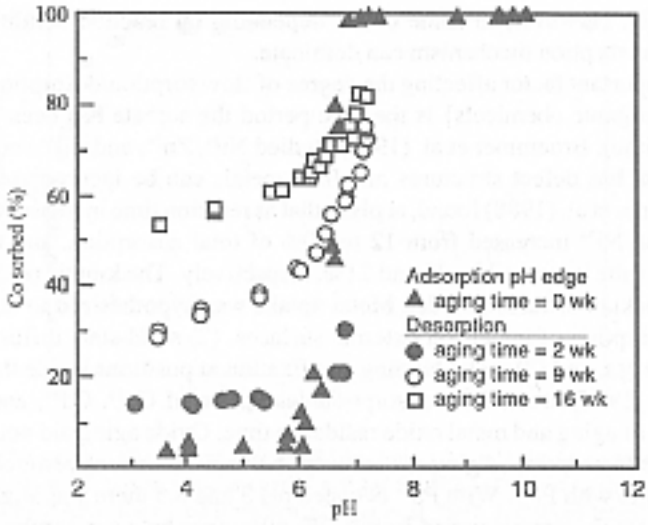

Fig. 4.19 Fractional adsorption of Co^{2+} to hydrous Fe-oxide (HFO) as a function of pH and HFO-Co^{2+} aging time [Reprinted from Ainsworth et al., 1994. Soil Sci. Soc. Am. J. 58:1615-1623 with permission of the Soil Science Society of America]

explained as slow diffusion of the As to or from interior surface complexation sites that exist within disordered aggregates of crystallites. The kinetic reactions could be described using a Fickian diffusion model.

Slow metal sorption/desorption has also been ascribed to conversion of the metal sorbate from a high to a low energy state (Kuo and Mikkelsen, 1980; Padmanabham, 1983; Schultz et al., 1987; Backes et al., 1995). Lehmann and Harter (1984) measured the kinetics of chelate-promoted Cu^{2+} release from a soil to assess the strength of the bond formed. Sorption/desorption was biphasic, which was attributed to high and low energy bonding sites. With increased residence time from 30 min to 24 h, Lehmann and Harter (1984) speculated that there was a transition of Cu from low to higher energy sites (as evaluated by release kinetics). Incubations for up to four days showed a continued uptake of Cu and a decrease in the fraction released within the first 3 min, which was referred to as the low energy sorbed fraction.

Recent studies using surface spectroscopic and microscopic techniques such as XAFS, electron paramagnetic resonance spectroscopy (EPR), X-ray photoelectron spectroscopy (XPS), auger electron spectroscopy (AES), scanning electron microscopy (SEM) and atomic force microscopy (AFM) have shown that the formation of polynuclear surface species (e.g., surface precipitates) on natural materials is an important sorption mechanism (Charlet and Manceau, 1993; Fendorf et al., 1994; Junta and Hochella, 1994; O'Day et al., 1994a,b; Wersin et al., 1994; Scheidegger et al., 1996, 1997, 1998; Towle et al., 1997).

Surface precipitates of Co, Cr(III), Cu, and Ni on oxides and aluminosilicates have been observed at metal surface loadings far below a theoretical monolayer coverage, and in a pH range well below the pH where the formation of metal hydroxide precipitates would be expected according to the thermodynamic solubility product (Charlet and Manceau, 1992; Fendorf et al., 1994; O'Day et al., 1994a,b, 1996; Scheidegger et al., 1996, 1997, 1998; Towle et al., 1997; Xia et al., 1997).

Three different types of polynuclear surface species have been proposed. Formation or sorption of polymers (dimers, trimers, etc.) on the surface as (1) a solid solution or coprecipitate that involves co-

ions dissolved from the adsorbent, (2) a precipitate formed on the surface composed of ions from the bulk solution, or (3) their hydrolysis products (Farley et al., 1985; Sposito, 1986; Brown, 1990; Chisholm-Brause et al., 1990; Scheidegger et al., 1996b).

Recent studies have shown that the formation of polynuclear surface species could be a significant cause of slow metal sorption on soil surfaces (Scheidegger et al., 1997, 1998). Such polynuclear surface species do not seem to occur with larger metals such as Pb^{2+} at surface loadings where such species have been observed with smaller metals such as Co^{2+}, Cu^{2+} and Ni^{2+} (Strawn and Sparks, unpublished data). This appears to be related to the mismatch in size between Pb^{2+} (1.19Å), and Al^{3+} (0.535Å) that is contained in the structure of the clay minerals and Al oxides. The Pb^{2+} ion is too large to fit into the mineral structure, while ions such as Ni^{2+} (0.69Å) and Co^{2+} (0.65Å) can.

Initial research with clay mineral systems demonstrated the formation of surface precipitates using XAFS spectroscopy, but the polynuclear structure was not strictly identified (O'Day et al., 1994a,b). Thus, the exact mechanism for surface precipitate formation remained unknown. Recent research in our laboratory suggests that during sorption of metals such as Ni, dissolution of the clay mineral or Al oxide surface leads to precipitation of mixed Ni/Al hydroxide surface species at the mineral/water interface (de la Caillerie et al., 1995; Scheidegger et al., 1996a, 1997, 1998). The precipitates are structurally similar to the mineral takovite (Scheidegger et al., 1997) or synthetic layered double hydroxides (de la Caillerie et al., 1995).

In general, the formation of surface precipitates has been considered a slow phenomenon. However, Scheidegger et al. (1998) have demonstrated that the rate of surface precipitate formation can be quite rapid. The appearance of surface precipitates during sorption of Ni to pyrophyllite at pH 7.5 occurred over time scales less than one hour. Similar results were observed for Ni sorption to kaolinite. However, the kinetics of Ni sorption onto gibbsite, and subsequent surface precipitate formation, were slower than for pyrophyllite (Figs. 4.16 and 4.20). Time resolved XAFS studies

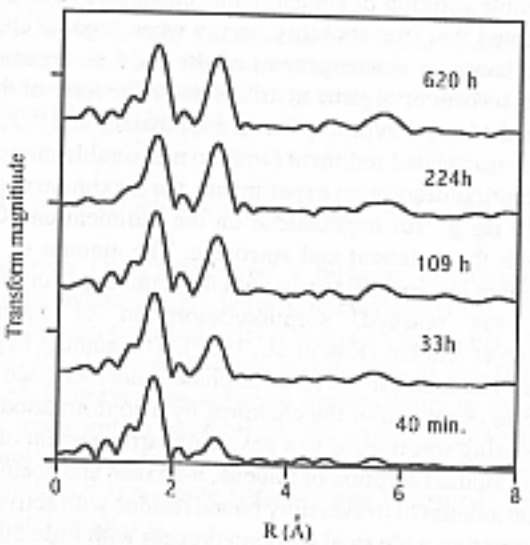

Fig. 4.20 Radial structure functions for Ni sorption to gibbsite for reaction times up to 620 h demonstrating the appearance and growth of second shell contributions due to surface precipitation and growth of a hydrotalcite-like phase [Reprinted from Scheidegger et al., 1998. The kinetics of mixed Ni-Al hydroxide formation on clays and aluminum oxide. Geochim. Cosmochim. Acta 62:2233-2245 with kind permission of Elsevier Science, Amsterdam, Netherlands]

demonstrated continued growth of the surface precipitate during Ni uptake as the structure and Ni:Al stoichiometry of the sorption complex approached that of a takovite-like phase (Scheidegger et al., 1998).

4.5.1.2 Organic Contaminants

Numerous studies on the kinetics of organic chemical sorption/desorption reactions on soils and soil components have shown that sorption/desorption is characterized by a rapid, reversible stage followed by a much slower, nonreversible stage (Karickhoff et al., 1979; DiToro and Horzempa, 1982; Karickhoff and Morris, 1985; Kan et al., 1997), or biphasic kinetics. The rapid phase has been ascribed to retention of the organic chemical in a labile form that is easily desorbed. However, the much slower reaction phase involves the entrapment of the chemical in a nonlabile form that is difficult to desorb. The labile form of the chemical is available for microbial attack, while the nonlabile portion is resistant to biodegradation.

This slower sorption/desorption reaction has been ascribed to intraparticle and interparticle diffusion of the chemical into organic matter and inorganic soil components (Wu and Gschwend, 1986; Steinberg et al., 1987; Ball and Roberts, 1991). Weber and Huang (1996) and Werth and Reinhard (1997) theorize that the slow intraparticle diffusion into SOM can be ascribed to the soft amorphous humic materials and the hard condensed microcrystalline materials. Cornelissen et al. (1997), who studied the temperature dependence of slow adsorption and desorption kinetics of some chlorobenzenes, polychlorinated biphenyls (PCBs) and polycyclic aromatic hydrocarbons (PAHs) in laboratory and field contaminated sediments, obtained activation enthalpies of 60–70 kJ mol^{-1} which are in the range for diffusion in polymers. These values are much higher than those for pore diffusion (20–40 kJ mol^{-1}) suggesting that intraorganic matter diffusion may be a more important mechanism for slow organic chemical sorption than interparticle pore diffusion.

However, some investigators have recently questioned the hypothesis that diffusion processes are responsible for the irreversible sorption of some organic chemicals (Kan et al., 1997; Chang et al., 1997). Kan et al. (1997) noted that irreversibility occurs when organic chemicals sorb on organic materials and the sorption causes a rearrangement of the solid or organic C matrix. Subsequent desorption from the altered sorbent or organic matrix is not the reverse of the sorption process. Kan et al. (1997) studied repeated adsorption/desorption of naphthalene and 2,2',5,5'-tetrachlorobiphenyl on a sediment and an antase surrogated sediment (with no measurable microporosity) amended with a surfactant. In repeated sorption/desorption experiments, the maximum concentrations that resisted desorption (q^{irr}_{max}) were 10 μg g^{-1} for naphthalene on the sediment and 0.36 μg g^{-1} for 2,2',5,5'-tetrachlorobiphenyl on both the sediment and surrogate. The amount of organic chemical in the irreversibly sorbed component increased linearly with the number of sorption steps until q^{irr}_{max} was reached. After q^{irr}_{max} was reached, sorption/desorption of naphthalene and 2,2',5,5'-tetrachlorobiphenyl became reversible (Kan et al., 1997). The authors hypothesized that since the concentration of the organic chemicals in the solution phase is not increased with desorption time, the irreversibility may be due to occlusion of the chemical by a conformation change in the organic C associated with the solid during sorption, or to a physical rearrangement of the organic C phase.

Chang et al. (1997) who studied sorption of toluene, *n*-hexane and acetone on pressed humic acid disks found an insignificant amount of irreversibly bound residue with activation energies in the range of 42.3–65.8 kJ mol^{-1}, suggesting a physical sorption process with little diffusion.

An example of the biphasic kinetics that is observed for many organic chemical reactions in soils/sediments is shown in Fig. 4.21. In this study, 55% of the labile polychlorinated biphenyl (PCB) was desorbed from sediments in a 24-h period, while little of the remaining 45% nonlabile fraction was

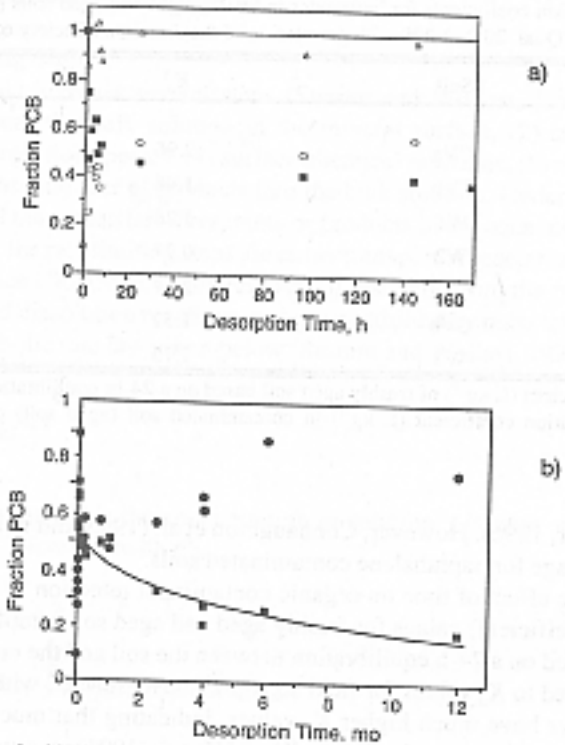

Fig. 4.21 (a) Short-term polychlorinated biphenyl (PCB) desorption in hours (h) from Hudson River sediment contaminated with 25 mg kg^{-1} PCB. Distribution of the PCB between the sediment (■) and XAD-4 resin (o) is shown, as well as the overall mass balance (Δ). The resin acts as a sink to retain the PCB that is desorbed (Carroll et al., 1994). (b) Long-term PCB desorption in months (mo) from Hudson River sediment contaminated with 25 mg kg^{-1} PCB. Distribution of the PCB between the sediment (■) and XAD-4 resin (•) is shown. The line represents a nonlinear regression of the data by a two-site model [Reprinted with permission from Carroll et al., 1994. Environ. Sci. Technol. 28:253-258. Copyright American Chemical Society]

desorbed in 170 h (Fig. 4.21a). Over another 1-yr period, ~ 50% of the remaining nonlabile fraction desorbed (Fig. 4.21b).

Pavlostathis and Mathavan (1992) observed a biphasic desorption process for field soils contaminated with trichloroethylene (TCE), tetrachloroethylene (PCE), toluene (TOL) and xylene (XYL). A fast desorption reaction occurred in 24 h followed by a much slower desorption reaction beyond 24 h. In 24 h, 9–29%, 14–48%, 9–40%, and 4–37% of the TCE, PCE, TOL, and XYL, respectively, were released. However, the apparent irreversibility or hysteresis may be an artifact caused by not reaching a true sorption equilibrium. For example, DiVincenzo and Sparks (1997), studying pentachlorophenol sorption/desorption on a soil, found that if desorption was initiated after an apparent sorption equilibrium (i.e., slow sorption was measured) was reached, hysteresis or irreversibility was significantly reduced.

A number of studies have also shown that with aging the nonlabile portion of the organic chemical in the soil/sediment becomes more resistant to release (McCall and Agin, 1985; Steinberg et al., 1987; Pignatello and Huang, 1991; Pavlostathis and Mathavan, 1992; Scribner et al., 1992; Alexander,

Table 4.4 Sorption distribution coefficients for herbicides in freshly aged and aged soils [Adapted from Pignatello and Huang, 1991. J. Environ. Qual. 20:222-228 with permission of the American Society of Agronomy]

Herbicide	Soil	K_d[1]	K_{app}[2]
		L kg^{-1}	
Metolachlor	CVa	2.96	39
	CVb	1.46	27
	W1	1.28	49
	W2	0.77	33
Atrazine	CVa	2.17	28
	CVb	1.32	29
	W3	1.75	4

[1] Sorption distribution coefficient (L kg^{-1}) of freshly aged soil based on a 24-hr equilibration period.
[2] Apparent sorption distribution coefficient (L kg^{-1}) in contaminated soil (aged soil) determined using a 24-hr equilibration period.

1995; Loehr and Webster, 1996). However, Connaughton et al. (1993) did not observe the nonlabile fraction increasing with age for naphthalene contaminated soils.

One way to gauge the effect of time on organic contaminant retention in soils is to compare K_d (sorption distribution coefficient) values for freshly aged and aged soil samples. In most studies, K_d values are measured based on a 24-h equilibration between the soil and the organic chemical. When these values are compared to K_d values for field soils previously reacted with the organic chemical (aged samples), the latter have much higher K_d values, indicating that much more of the organic chemical is in a sorbed state. For example, Pignatello and Huang (1991) measured K_d values in freshly aged (K_d) and "aged" soils (K_{app}, apparent sorption distribution coefficient) reacted with atrazine and metolachlor, two widely used herbicides. The aged soils had been treated with the herbicides 15–62 months before sampling. The K_{app} values ranged from 2.3–42 times higher than the K_d values (Table 4.4).

Scribner et al. (1992) studying simazine (a widely used triazine herbicide for broadleaf and grass control in crops) desorption and bioavailability in aged soils found that K_{app} values were 15 times higher than K_d values. Scribner et al. (1992) also showed that 48% of the simazine added to the freshly aged soils was biodegradable over a 34-day incubation period while none of the simazine in the aged soil was biodegraded.

One of the implications of these results is that while many transport and degradation models for organic contaminants in soils and waters assume that the sorption process is an equilibrium process, the above studies clearly show that kinetic reactions must be considered when making predictions about the mobility and fate of organic chemicals. Moreover, calculation of K_d values based on a 24-h equilibration period, which are commonly used in fate and risk assessment models, can be inaccurate since 24-h K_d values often overestimate the amount of organic chemical in the solution phase.

The finding that many organic chemicals are quite persistent in the soil environment has both good and bad features. The beneficial aspect is that the organic chemicals are less mobile and may not be readily transported in groundwater supplies. The negative aspect is that their persistence and inaccessibility to microbes may make decontamination more difficult, particularly if *in situ* remediation techniques such as biodegradation are employed.

4.5.2 Kinetics of Mineral Dissolution

4.5.2.1 Rate Limiting Steps

Dissolution of minerals involves several steps (Stumm and Wollast, 1990): (1) mass transfer of dissolved reactants from the bulk solution to the mineral surface, (2) adsorption of solutes, (3) interlattice transfer of reaction species, (4) surface chemical reactions, (5) removal of reactants from the surface, and (6) mass transfer of products into the bulk solution. Under field conditions mineral dissolution is slow and mass transfer of reactants or products in the aqueous phase (Steps 1 and 6) is not rate limiting. Thus, the rate limiting steps are either transport of reactants and products in the solid phase (Step 3) or surface CRs (Step 4) and removal of reactants from the surface (Step 5).

Transport controlled dissolution reactions or those controlled by mass transfer or diffusion can be described using a parabolic rate law given below (Stumm and Wollast, 1990):

$$r = \frac{dC}{dt} = kt^{-1/2} \qquad [4.17]$$

where r is the reaction rate, C is the concentration in solution, t is time, and k is the reaction rate constant. Integrating, C increases with $t^{1/2}$.

$$C = C_0 + 2kt^{1/2} \qquad [4.18]$$

where C_0 is the initial concentration in solution.

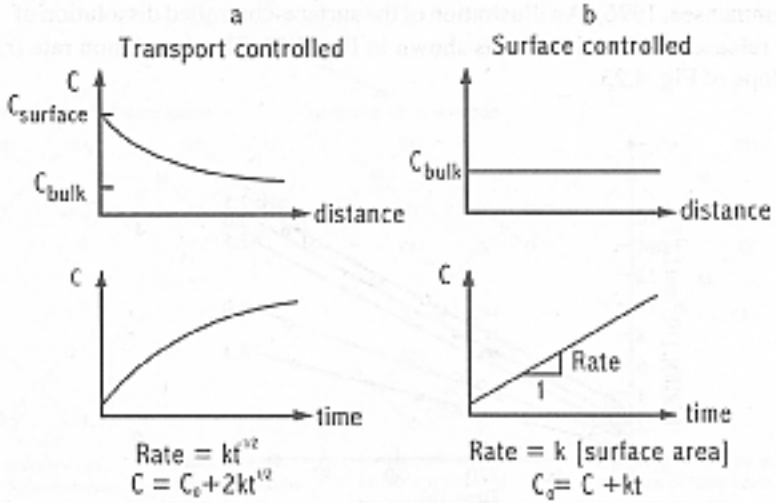

Fig. 4.22 Transport versus surface-controlled dissolution. Schematic representation of concentration in solution, C, as a function of distance from the surface of the dissolving mineral. In the lower part of the figure, the change in concentration is given as a function of time [Reprinted from Stumm, 1992. Chemistry of the solid-water interface. with permission of John Wiley & Sons, Inc.].

If the surface reactions are slow compared to the transport reactions, dissolution is surface controlled, which is the case for most dissolution reactions of silicates and oxides. In surface-controlled reactions, the concentrations of solutes next to the surface are equal to the bulk solution concentrations and the dissolution kinetics are zero order if steady-state conditions are operational on the surface. Thus, the dissolution rate (r) is

$$r = \frac{dC}{dt} = kA \qquad [4.19]$$

and r is proportional to the mineral's surface area, A. Thus, for a surface-controlled reaction the relationship between t and C should be linear. Fig. 4.22 compares transport- and surface-controlled dissolution mechanisms.

Intense arguments have ensued over the years concerning the mechanism for mineral dissolution. Those that supported a transport-controlled mechanism believed that a leached layer formed as mineral dissolution proceeded and that subsequent dissolution took place by diffusion through the leached layer (Wollast, 1967; Petrovic et al., 1976). Advocates of this theory found that dissolution was described by the parabolic rate law (Equation [4.18]). However, the apparent transport-controlled kinetics may be an artifact caused by dissolution of hyperfine particles formed on the mineral surfaces after grinding that are highly reactive sites, or by use of batch methods that cause reaction products to accumulate causing precipitation of secondary minerals. These experimental artifacts can cause incongruent reactions and pseudoparabolic kinetics. Studies employing XPS and nuclear resonance profiling (Schott and Petit, 1987; Casey et al., 1989) have demonstrated that, although some incongruency may occur in the initial dissolution process, which may be diffusion controlled, the overall reaction is surface controlled. Energies of activation from 60–86 kJ mol^{-1} have been observed for dissolution of oxides and silicates, further suggesting surface-controlled dissolution (Lasaga, 1984; Jordan and Rammensee, 1996). An illustration of the surface-controlled dissolution of γ-Al_2O_3 resulting in a linear release of Al^{3+} with time is shown in Fig. 4.23. The dissolution rate (r) can be obtained from the slope of Fig. 4.23.

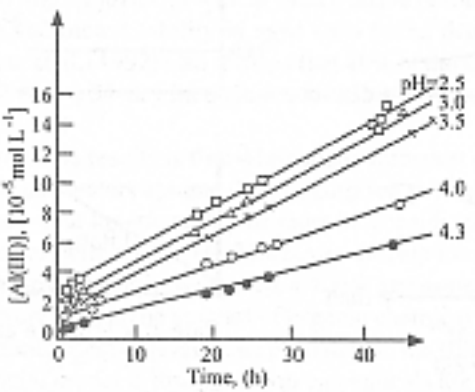

Fig. 4.23 Linear dissolution kinetics observed for the dissolution of γ-Al_2O_3. Representative of processes whose rates are controlled by a surface reaction and not by transport [Reprinted from Furrer and Stumm, 1986. The coordination chemistry of weathering. Geochim Cosmochim. Acta 50:1847-1860 with kind permission of Elsevier Science, Amsterdam, Netherlands]

Scanning force microscopy (SFM) which has also been used increasingly as an *in situ* technique for imaging mineral surfaces immersed in aqueous solution during the course of dissolution (Hellman et al., 1992; Hillner et al., 1992a,b; Johnsson et al., 1992; Bosbach and Rammensee, 1994; Maurice et al., 1995) permits a direct measure of surface-controlled dissolution rates by providing 3-dimensional data on changes in microtopography. *In situ* SFM has the unique ability to detect separate processes, such as dissolution and secondary phase formation, occurring simultaneously on a mineral surface (Maurice, 1997).

4.5.2.2 Surface-Controlled Dissolution Mechanisms

Dissolution of oxide minerals through a surface-controlled reaction by ligand and proton promoted processes has been described by Furrer and Stumm (1986), Zinder et al. (1986), and Stumm and Furrer (1987) using a surface coordination approach. The important reactants in these processes are H_2O, H^+, OH^-, ligands, and reductants and oxidants. The reaction mechanism occurs in two steps (Stumm and Wollast, 1990):

$$\text{Surface sites} + \text{Reactants}\left(H^+, OH^-, \text{ligands}\right) \xrightarrow{\text{fast}} \text{Surface species} \qquad [4.20]$$

$$\text{Surface species} \xrightarrow[\text{detachment of metal(M)}]{\text{slow}} M(aq) \qquad [4.21]$$

Thus, the attachment of the reactants to the surface sites is fast and detachment of metal species from the surface into solution is slow and rate limiting.

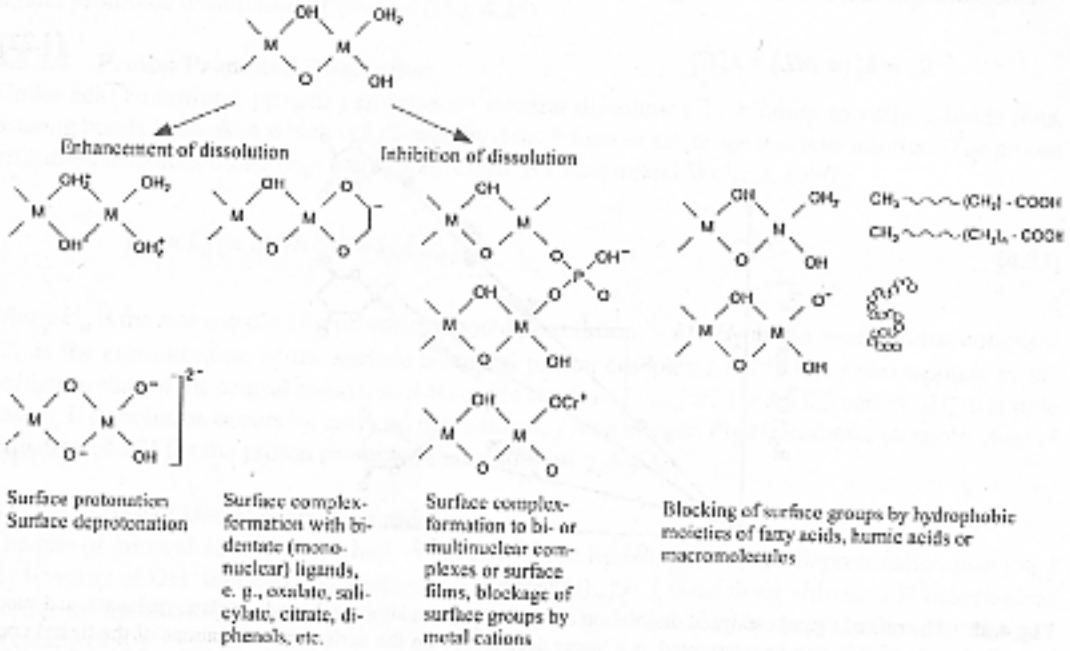

Fig. 4.24 The dependence of surface reactivity and of kinetic mechanisms on the coordinative environment of the surface groups [Reprinted from Stumm and Wollast, 1990. Rev. Geophys. 28:53-69, with permission]

4.5.2.3 Ligand Promoted Dissolution

Fig. 4.24 shows how the surface chemistry of the mineral affects dissolution. One sees that surface protonation of the surface ligand increases dissolution by polarizing interatomic bonds close to the central surface ions that promote the release of a cation surface group into solution. Hydroxyls that bind to surface groups at higher pHs can ease the release of an anionic surface group into the solution phase.

Ligands that form surface complexes by ligand exchange with a surface hydroxyl add negative charge to the Lewis acid center coordination sphere, and lower the Lewis acid acidity. This polarizes the M-O bonds causing detachment of the metal cation into the solution phase. Thus, innersphere surface complexation plays an important role in mineral dissolution. Ligands such as oxalate, salicylate, F^-, EDTA, and NTA increase dissolution, but others, such as SO_4^{2-}, CrO_4^{2-} and benzoate, inhibit dissolution. Phosphate, arsenate, and selenite enhance dissolution at low pH and dissolution is inhibited at pH > 7 (Bondietti et al., 1993).

The reason for these differences may be that bidentate species that are mononuclear promote dissolution while binuclear bidentate species inhibit dissolution. With binuclear bidentate complexes, more energy may be needed to remove two central atoms from the crystal structure. With phosphate and arsenate, at low pH, mononuclear species are formed while at higher pH (~ pH 7), binuclear or trinuclear surface complexes form. Mononuclear bidentate complexes are formed with oxalate while binuclear bidentate complexes form with CrO_4^{2-}. Additionally, the electron donor properties of CrO_4^{2-} and oxalate are also different. With CrO_4^{2-}, a high redox potential is maintained at the oxide surface which restricts reductive dissolution (Stumm and Wollast, 1990; Stumm, 1992). Dissolution can also be inhibited by cations such as VO^{2+}, Cr(III) and Al(III) that block surface functional groups (Bondietti et al., 1993).

One can express the rate of the ligand promoted dissolution (R_L) as:

$$R_L = k'_L(=ML) = k'_L C'_L \qquad [4.22]$$

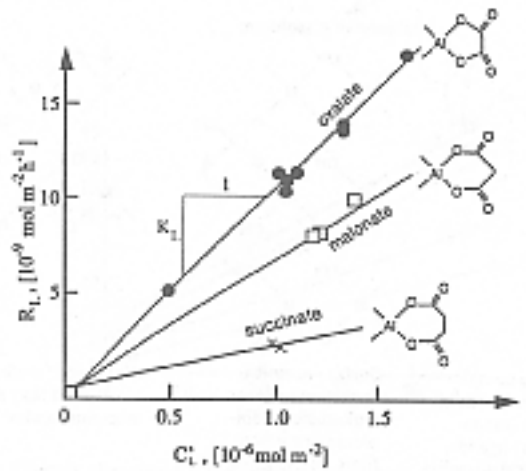

Fig. 4.25 The rate of ligand catalyzed dissolution of γ-Al_2O_3 by the aliphatic ligands oxalate, malonate, and succinate, R_L (nmol m^{-2} h^{-1}), can be interpreted as a linear dependence on the surface concentrations of the ligand complexes, C'_L. In each case the individual values for C'_L were determined experimentally [Reprinted from Furrer and Stumm, 1986. The coordination chemistry of weathering. Geochim. Cosmochim. Acta 50:1847-1860 with kind permission of Elsevier Science, Amsterdam, Netherlands].

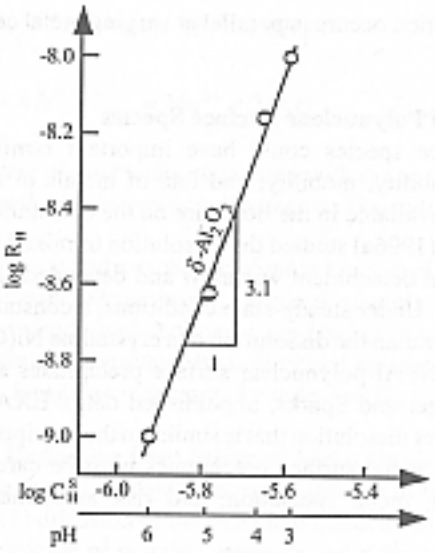

Fig. 4.26 The dependence of the rate of proton promoted dissolution of γ-Al_2O_3, R_H (mol m^{-2} h^{-1}), on the surface concentration of the proton complexes, C^s_H (mol m^{-2}). [Reprinted from Furrer and Stumm, 1986. The Coordination chemistry of weathering. Geochim Cosmochim. Acta 57:2271-2282 with kind permission of Elsevier Science, Amsterdam, Netherlands]

where k'_L is the rate constant for ligand promoted dissolution (t^{-1}), $\equiv ML$ is the metal-ligand complex, and C^s_L is the surface concentration of the ligand (mol m^{-2}). Equation [4.22] adequately describes ligand promoted dissolution of γ-Al_2O_3 (Fig. 4.25).

4.5.2.4 Proton Promoted Dissolution

Under acid conditions, protons can promote mineral dissolution by binding to surface oxide ions, causing bonds to weaken which is followed by detachment of metal species into solution. The proton promoted dissolution rate (R_H) can be expressed as (Stumm and Wollast, 1990):

$$R_H = k'_H\left(\equiv MOH_2^+\right)^j = k'_H\left(C^s_H\right)^j \qquad [4.23]$$

where k'_H is the rate constant for proton promoted dissolution, $\equiv MOH_2^+$ is the metal-proton complex, C^s_H is the concentration of the surface adsorbed proton complex (mol^{-2}) and j corresponds to the oxidation state of the central metal ion in the oxide structure (i.e., $j = 3$ for Al(III) and Fe(III) in simple cases). If dissolution occurs by only one mechanism, j is an integer. Fig. 4.26 shows an application of Equation [4.23] for the proton promoted dissolution of γ-Al_2O_3.

4.5.2.5 Overall Dissolution Mechanisms

The rate of mineral dissolution, which is the sum of the ligand, proton, and deprotonation promoted (or bonding of OH^- ligands) dissociation [$R_{OH} = k'_{OH}\left(C^s_{OH}\right)^j$] rates along with the pH independent portion of the dissolution rate $\left(k'_{H_2O}\right)$ which is due to hydration, can be expressed as (Stumm and Wollast, 1990):

$$R = k'_L\left(C^s_L\right) + k'_H\left(C^s_H\right)^j + k'_{OH}\left(C^s_{OH}\right)^j + k'_{H_2O} \qquad [4.24]$$

Equation [4.24] is valid if dissolution occurs in parallel at varying metal centers (Furrer and Stumm, 1986).

4.5.2.6 Dissolution Kinetics of Polynuclear Surface Species

While polynuclear metal surface species could have important ramifications with respect to environmental quality (bioavailability, mobility, and fate of metals in soils and waters) through dissolution, little information is available in the literature on the dissolution kinetics of polynuclear species. Scheidegger and Sparks (1996a) studied the dissolution of mixed Ni-Al polynuclear surface species from pyrophyllite. Nickel detachment was slow and depended strongly on the pH and the experimental method (Fig. 4.27). Under steady-state conditions, a constant Ni detachment rate was observed, which was much slower than the dissolution of a crystalline $Ni(OH)_2$ reference compound.

The structures of the mixed Ni-Al polynuclear surface precipitates are also not changed after extensive dissolution (Scheidegger and Sparks, unpublished data). EXAFS analysis shows that a tacovite-like structure remains after dissolution that is similar to the precipitate before commencement of dissolution. It is obvious that metal surface precipitates must be carefully considered in metal surface complexation modeling, metal speciation, and risk assessments for the migration of contaminants in polluted sites.

4.5.3 Redox Kinetics

It is well-known that Mn (III/IV), Fe(III), Co(III), and Pb(IV) oxides/hydroxides are thermodynamically stable in oxygenated systems at neutral pH. However, under anoxic conditions, reductive dissolution of oxides/hydroxides by reducing agents occurs as shown below for MnOOH and MnO_2 (Stone, 1991):

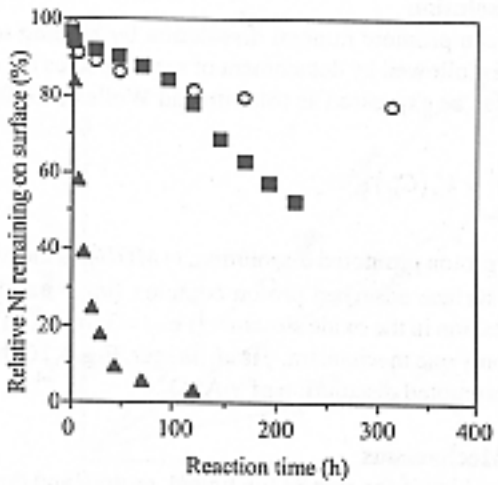

Fig. 4.27 Kinetics of Ni detachment from surface precipitates at pH = 4. Relative Ni remaining on the surface (%) is shown for the *conventional method* (○) and the *replenishment method* (■) as a function of the reaction time. 98% of the initial Ni was sorbed in the beginning of the detachment experiment. The dissolution of an equivalent amount of crystalline $Ni(OH)_2$ (in mol) at pH = 4 is given for comparison (▲) [Reprinted from Scheidegger and Sparks (1996a). Chem. Geol. 132:157-164, with permission].

$$Mn(III)OOH(s) + 3H^+ + e^- = Mn^{2+} + 2H_2O \qquad E^0 = +1.50V \qquad [4.25]$$

$$Mn(IV)O_2(s) + 4H^+ + 2e^- = Mn^{2+} + 2H_2O \qquad E^0 = +1.23V \qquad [4.26]$$

Changes in the oxidation state of the metals associated with the oxides above can greatly affect their solubility and mobility in soil and aqueous environments. The reductants can be either inorganic or organic.

There are a number of natural and xenobiotic organic functional groups that are good reducers of oxides and hydroxides. These include carboxyl, carbonyl, phenolic, and alcoholic functional groups of SOM. Microorganisms in soils and sediments are also examples of organic reductants. Stone (1987a) showed that oxalate and pyruvate, two microbial metabolites, could reduce and dissolve Mn(III/IV) oxide particles. Inorganic reductants include As(III), Cr(III), and Pu(III).

4.5.3.1 Mechanisms for Reductive Dissolution of Metal Oxides/Hydroxides

The reductive dissolution of metal oxides/hydroxides appears to occur in the following sequential steps (Stone, 1986; 1991): (1) diffusion of the reductant molecules to the oxide surface, (2) a surface chemical reaction, and (3) release of reaction products and diffusion away from the oxide surface. Steps (1) and (3) are transport steps. The rate-controlling step in reductive dissolution of oxides appears to be surface chemical reaction control. Reductive dissolution can be described by both inner- and outersphere complex mechanisms that involve (1) precursor complex formation, (2) electron transfer, and (3) breakdown of the successor complex (Fig. 4.28). Innersphere and outersphere precursor complex formation are adsorption reactions that increase the density of reductant molecules at the oxide surface which promotes electron transfer (Stone, 1991). In the innersphere mechanism, the reductant enters the inner coordination sphere by ligand exchange and bonds directly to the metal center prior to electron transfer. With the outersphere complex, the inner coordination sphere is left intact and electron transfer is enhanced by an outersphere precursor complex (Stone, 1986). Kinetic studies have shown that high rates of reductive dissolution are favored by high rates of precursor complex formation (i.e., large k_1 and low k_{-1} values), high electron transfer rates (i.e., large k_2), and high rates of product release (i.e., high k_3) (Fig. 4.28).

Specifically adsorbed cations and anions may reduce reductive dissolution rates by blocking oxide surface sites or by causing release of Mn(II) into solution. Stone and Morgan (1984a) showed that PO_4^{3-} inhibited the reductive dissolution of Mn(III/IV) oxides by hydroquinone. Addition of 10^{-3} *M*

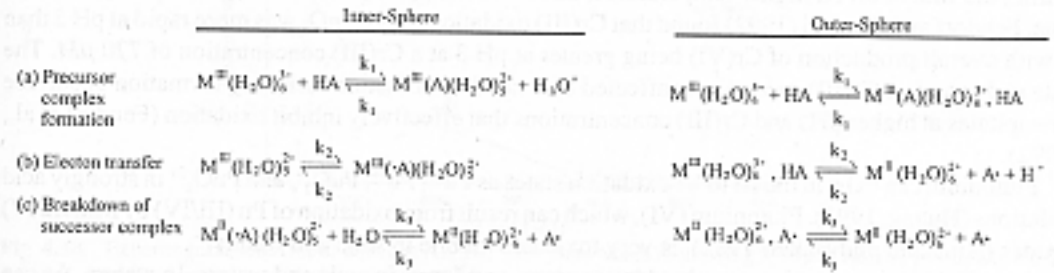

Fig. 4.28 Reduction of $M(H_2O)_6^{3+}$ by phenol (HA) in homogeneous solution [From Stone, 1986. ACS Symp. Ser 323:446-461 with permission of the American Chemical Society]

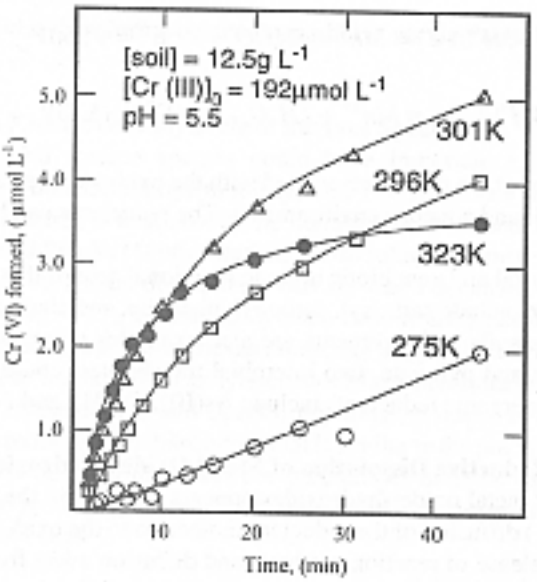

Fig. 4.29 Effect of temperature on the kinetics of Cr(III) oxidation in moist Hagerstown silt loam soil [From Amacher and Baker, 1982]

PO_4^{3-} at pH 7.68 caused the dissolution rate to be only 25% of the rate when PO_4^{3-} was not present. Phosphate had a greater effect than Ca^{2+}.

4.5.3.2 Oxidation of Pollutants

As mentioned earlier, Mn oxides can oxidize a number of environmentally important ions that can be toxic to humans and animals. Chromium and plutonium are similar in their chemical behavior in aqueous settings (Rai and Serne, 1977; Bartlett and James, 1979). They can exist in multiple oxidation states and as both cationic and anionic species. Chromium (III) is quite stable and innocuous, and occurs as Cr^{3+} and its hydrolysis products or as CrO_2^-. Chromium (III) can be oxidized to Cr(VI) by Mn(III/IV) oxides (Bartlett and James, 1979; Fendorf and Zasoski, 1992). Chromium(VI) is mobile in the soil environment and is a suspected carcinogen. It occurs as the dichromate ($Cr_2O_7^{2-}$) or chromate ($HCrO_4^-$ and CrO_4^{2-}) anions (Huang, 1991).

Fig. 4.29 shows the oxidation kinetics of Cr(III) to Cr(VI) in a soil. Most of the oxidation occurred during the first hour. At higher temperatures, there was a rapid oxidation rate, followed by a slower rate. Fendorf and Zasoski (1992) found that Cr(III) oxidation on δ-MnO_2 was more rapid at pH 5 than 3 with overall production of Cr(VI) being greater at pH 3 at a Cr(III) concentration of 770 μM. The rate and extent of Cr(III) oxidation is affected by a number of factors including formation of surface precipitates at higher pHs and Cr(III) concentrations that effectively inhibit oxidation (Fendorf et al., 1992).

Plutonium can exist in the III to VI oxidation states as Pu^{3+}, Pu^{4+}, PuO_2^+, and PuO_2^{2+} in strongly acid solutions (Huang, 1991). Plutonium (VI), which can result from oxidation of Pu (III/IV) by Mn(III/IV) oxides (Amacher and Baker, 1982), is very toxic and mobile in soils and waters.

Arsenic (As) can exist in several oxidation states and forms in soils and waters. In waters, As can exist in the +5, +3, 0, and −3 oxidation states. Arsenite, As(III), and arsine (AsH_3, where the oxidation

state of As is –3) are much more toxic to humans than arsenate, As(V). Manganese (III/IV) oxides can oxidize As(III) to As(V) as shown below where As(III) as $HAsO_2$ is added to MnO_2 to produce As(V) as H_3AsO_4 (Oscarson et al., 1983):

$$HAsO_2 + MnO_2 = (MnO_2)\cdot HAsO_2 \quad [4.27]$$

$$(MnO_2)\cdot HAsO_2 + H_2O = H_3AsO_4 + MnO \quad [4.28]$$

$$H_3AsO_4 = H_2AsO_4^- + H^+ \quad [4.29]$$

$$H_2AsO_4^- = HAsO_4^{2-} + H^+ \quad [4.30]$$

$$(MnO_2)HAsO_2 + 2H^+ = H_3AsO_4 + Mn^{2+} \quad [4.31]$$

Equation [4.28] involves the formation of an adsorbed layer. Oxygen transfer occurs and $HAsO_2$ is oxidized to H_3AsO_4 (Equation [4.28]). At pH ≤ 7, the predominant As(III) species is arsenious acid ($HAsO_2$), but the oxidation product, H_3AsO_4, will dissociate and form the same quantities of $H_2AsO_4^-$ and $HAsO_4^{2-}$ with little H_3AsO_4 present at equilibrium (Eqs. 4.29 and 4.30). Each mole of As(III) oxidized releases about 1.5 mol H^+. The H^+ produced after H_3AsO_4 dissociation reacts with the adsorbed $HAsO_2$ on MnO_2, forming H_3AsO_4, and leads to the reduction and dissolution of Mn(IV) (Equation [4.31]). Thus, every mole of As(II) that is oxidized to As(V) results in 1 mol of Mn(IV) in the solid phase being reduced to Mn(II) and partially dissolved in solution (Oscarson et al., 1981).

Oscarson et al. (1980) studied the oxidation of As(III) to As(V) in sediments from five lakes in Saskatchewan, Canada. Oxidation of As(III) to As(V) occurred within 48 hr. In general, > 90% of the added As was sorbed on the sediments within 72 hr. Scott and Morgan (1995) studied the oxidation of As(III) by synthetic birnessite. The depletion of As(III) was rapid with 50% of the initial As(III) removed from solution in 10 minutes and after 90 minutes the As(III) concentration was below the detection limit. Arsenic (V) was released into solution as fast as As(III) was depleted and the total

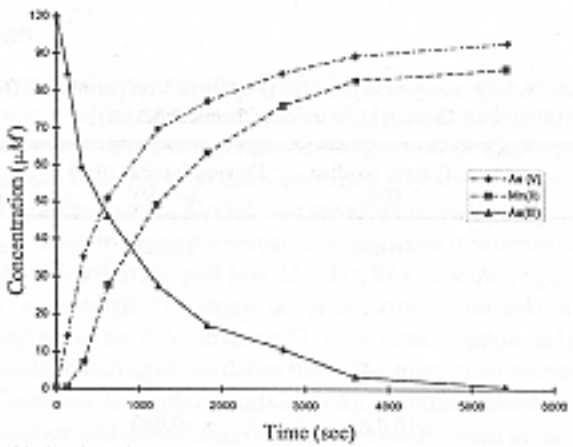

Fig. 4.30 Experimental behavior of aqueous As(III), As(V) and Mn(II) following 99.6 μM As(III) addition to a 0.21 g L^{-1} of γ-MnO_2 particle suspension at pH 4, 25 °C, and 0.1 M $NaClO_4$ [Reprinted with permission from Scott and Morgan, 1995. Environ. Sci. Technol. 29:1898-1905. Copyright American Chemical Society]

concentration of aqueous As was about constant over the duration of the experiment (Fig. 4.30). Scott and Morgan (1995) concluded that the process of electron transfer and release of As(V) were fast compared to the sorption of As(III), the rate limiting step.

Manganese oxides and hydroxides (e.g., Mn_3O_4 and MnOOH) may also catalyze the oxidation of other trace metals such as Co^{2+}, Co^{3+}, Cu^{2+}, Ni^{2+}, Ni^{3+}, and Pb^{2+} by disproportionation to Mn^{2+} and MnO_2 (Hem, 1978). The disproportionation results in vacancies in the Mn oxide structure. Since the Mn^{2+} and Mn^{3+} in the oxides have similar physical sizes as Co^{2+}, Co^{3+}, Cu^{2+}, Ni^{2+}, Ni^{3+}, and Pb^{2+}, these metals can occupy the vacancies in the Mn oxide and become part of the structure. With disproportionation or with other redox processes involving the Mn oxides, the solubility of the metals can be affected. For example, if during the disproportionation process Co_3O_4, the oxidized form of the metal forms from Co^{2+}, the reaction can be expressed as (Hem, 1978):

$$2Mn_3O_4(s)+3Co^{2+}+4H^+ \rightarrow MnO_2(s)+Co_3O_4(s)+5Mn^{2+}+2H_2O \qquad [4.32]$$

and the equilibrium constant (K°) is (Hem, 1978)

$$\left(Mn^{2+}\right)^5/\left(Co^{2+}\right)^3\left(H^+\right)^4 = 10^{18.33} \qquad [4.33]$$

Thus, the oxidation of Co(II) to Co(III) reduces its solubility and mobility in the environment. Using XPS analyses (Murray and Dillard, 1979), this reaction has been shown to occur. More recent evidence for heterogeneous redox reactions of trace metals is discussed in Section B, chapter 9. Scott and Morgan (1996) studied the oxidation of Se(IV) by synthetic birnessite. Se(IV) was oxidized to Se(VI) with Se(VI) first appearing in the aqueous suspension after 12 h and was produced at a constant rate over the duration of the experiment (28 days). Scott and Morgan (1996) suggested the following oxidation mechanism: (1) birnessite directly oxidized Se(IV) through a surface complex mechanism; (2) the rate limiting step in the production of Se(VI) was the electron transfer step involving a transfer of two electrons from the anion to the metal ion, breaking of two Mn-O bonds, and addition of an O

Table 4.5 Inorganic redox reactions with manganese dioxides [Reprinted with permission from Scott and Morgan, 1995. Environ. Sci. Technol. 29:1898-1905. Copyright American Chemical Society]

System	Time to oxidize 50%	Driving force at pH 4 Δe° (V)‡	Source
δ-MnO_2: As(III) → As(V) pH 4, 25 °C, 14 m^2 L^{-1}	10 min	+0.529	Scott and Morgan (1995)
δ-MnO_2: Se(IV) → Se(VI)			
pH 4, 35 °C, 14 m^2 L^{-1}	10 days		
pH 4, 25 °C, 28 m^2 L^{-1}	16 days	+0.092	
pH 4, 25 °C, 14 m^2 L^{-1}	30 days		
β-MnO_2: Cr(III) → Cr(VI) pH 4, 25 °C, 71 m^2 L^{-1}	95 days	+0.011	Eary and Rai (1987)

‡ The activity ratio for each oxidant/reductant pair is taken as unity.

from water to Se(VI); and (3) the reaction products Se(VI) and Mn(II) were released from the surface by different steps.

Scott and Morgan (1996) compared their results to those of Eary and Rai (1987) who studied Cr(III) oxidation by pyrolusite (β-MnO_2) between pH 3.0 and 4.7 and Scott and Morgan (1995) who studied As(III) oxidation by birnessite (δ-MnO_2) at pH values between 4.0 and 8.2 (Table 4.5). The Cr(III) redox transformation on pyrolusite was slowest which Scott and Morgan (1996) attributed to unfavorable adsorption on both a positively charged surface and aqueous species and the small thermodynamic driving force. Also, the transfer of three electrons from Cr(III) to Mn(IV) requires the involvement of more than one Mn(IV) atom per Cr(III) atom.

Manganese oxides also appear to play an important role in ligand facilitated metal transport. Using soil columns that consisted of fractured saprolite coated with amorphous Fe- and Mn-oxides, Jardine et al. (1993) studied the transport of Co(II) $EDTA^{2-}$, a mixture of Co(II) $EDTA^{2-}$ and Co(III) $EDTA^{-}$ and Sr $EDTA^{2-}$. The Mn-oxides oxidized Co(II)-$EDTA^{2-}$ into Co(III)-$EDTA^{-}$, a very stable complex (log K value of 41.4, Xue and Traina, 1996). The formation of this complex resulted in enhanced transport of Co.

Xue and Traina (1996) found that an aerobic goethite suspension catalyzed oxidation of Co(II) $EDTA^{2-}$ to Co(III)-$EDTA^{-}$ by dissolved O_2. The kinetics were described using a pseudo-first-order rate constant, k_1 of 0.0078 ± 0.0002 h^{-1} at pH 5 and a goethite concentration of 3.09 g L^{-1}.

A number of investigators have studied the reductive dissolution of Mn oxides by organic pollutants such as hydroquinone (Stone and Morgan, 1984a), substituted phenols (Stone, 1987b), and other organic compounds (Stone and Morgan, 1984b). With substituted phenols, the rate of dissolution was proportional to substituted phenol concentration and the rate increased as pH decreased (Stone, 1987b). Phenols containing alkyl, alkoxy, or other electron donating substituents were more slowly degraded; p-nitrophenol reacted slowly with Mn(III/IV) oxides. The increased rate of reductive dissolution at lower pH may be due to more protonation reactions that enhance the creation of precursor complexes or increases in the protonation level of the surface precursor complexes that increase electron transfer rates (Stone, 1987b). Further discussions on this topic can be found in Section B, Chapter 9.

4.6 Conclusions

Research on the kinetics and mechanisms of soil chemical reactions will be a common theme in soil and environmental sciences for decades to come. This research emphasis is in large part due to the need to more accurately understand and predict the long-term fate and transport of contaminants in the subsurface environment. Without such data, economically sound decisions about soil remediation cannot be made and risk assessment models are incomplete and most probably inaccurate.

While some very fine and informative research on rates and mechanisms of soil chemical reactions/processes has been conducted in the past few decades, there are many gaps that need to be filled. The following research is needed: (1) more accurate kinetic models that describe reactions on multireactive, heterogeneous particle surfaces; (2) long-term sorption and particularly, desorption rate studies; (3) a better understanding of residence time effects on plant nutrient, radionuclide, metal, and organic retention/release mechanisms on soils and other natural materials; (4) an increased knowledge of nucleation/precipitation and dissolution reaction rate phenomena at the mineral/water interface and their effect on nutrient/contaminant mobility and bioavailability in the soil environment; (5) more studies on the kinetics and mechanisms of redox processes in soils, particularly the role that soil components such as Mn oxides have on oxidation/reduction of inorganic and organic pollutants; and, (6) increased use of time resolved, *in situ* spectroscopic and microscopic techniques to confirm reaction mechanisms.

4.7 References

Aharoni, C. 1984. Kinetics of adsorption: The S shaped Z(t) plot. Adsorpt. Sci. Technol. 1:1–29.

Aharoni, C., and D.L. Sparks. 1991. Kinetics of soil chemical reactions: A theoretical treatment. p. 1–18. *In* D.L. Sparks and D.L. Suarez (ed.) Rates of soil chemical processes. Soil Sci. Soc. Am. Spec. Pub. 27, Soil Science Society of America, Madison, WI.

Aharoni, C., and Y. Suzin. 1982a. Application of the Elovich equation to the kinetics of occlusion: Part 1. Homogeneous microporosity. J. Chem. Soc. Farad. Trans. 178:2313–2320.

Aharoni, C., and Y. Suzin. 1982b. Application of the Elovich equation to the kinetics of occlusion: Part 3. Heterogeneous microporosity. J. Chem. Soc. Farad. Trans. 178:2329–2336.

Aharoni, C., and M. Ungarish. 1976. Kinetics of activated chemisorption. Part 1. The non-Elovichian part of the isotherm. J. Chem. Soc. Farad. Trans. 172:400–408.

Ainsworth, C.C., J.L. Pilou, P.L. Gassman, and W.G.V.D. Sluys. 1994. Cobalt, cadmium, and lead sorption to hydrous iron oxide: Residence time effect. Soil Sci. Soc. Am. J. 58:1615–1623.

Alexander, M. 1995. How toxic are toxic chemicals in soils? Environ. Sci. Technol. 29:2713–2717.

Allen, E.R., D.W. Ming, L.R. Hossner, and D.L. Henninger. 1995. Modeling transport kinetics in clinoptilolite-phosphate rock systems. Soil Sci. Soc. Am. J. 59:248–255.

Amacher, M.C. 1991. Methods of obtaining and analyzing kinetic data. p.19–59. *In* D.L. Sparks and D.L. Suarez (ed.) Rates of soil chemical processes. Soil Sci. Soc. Am. Spec. Pub. 27, Soil Science Society of America, Madison, WI.

Amacher, M.C., and D.E. Baker. 1982. Redox reactions involving chromium, plutonium, and manganese in soils. Pennsylvania State University, University Park, PA.

Atkinson, R.J., F.J. Hingston, A.M. Posner, and J.P. Quirk. 1970. Elovich equation for the kinetics of isotope exchange reactions at solid-liquid interfaces. Nature 226:148–149.

Backes, C.A., R.G. McLaren, A.W. Rate, and R.S. Swift. 1995. Kinetics of cadmium and cobalt desorption from iron and manganese oxides. Soil Sci. Soc. Am. J. 59:778–785.

Ball, W.P., and P.V. Roberts. 1991. Long-term sorption of halogenated organic chemicals by aquifer material: 1. Equilibrium. Environ. Sci. Technol. 25: 1223–1236.

Bartlett, R.J., and B.R. James. 1979. Behavior of chromium in soils. III. Oxidation. J. Environ. Qual. 8:31–35.

Bernasconi, C.F. 1976. Relaxation kinetics. Academic Press, New York, NY.

Bondietti, G., J. Sinniger, and W. Stumm. 1993. The reactivity of Fe(III) (hydr)oxides: Effects of ligands in inhibiting the dissolution. Colloid. Surf. A 79:157–167.

Bosbach, D., and W. Rammensee. 1994. *In situ* investigation of growth and dissolution on the (010) surface of gypsum by scanning force microscopy. Geochim. Cosmochim. Acta. 58:843–849.

Brown Jr., G.E. 1990. Spectroscopic studies of chemisorption reaction mechanisms at oxide-water interfaces. p. 309–353. *In* M.F. Hochella and A.F. White (ed.) Mineral-water interface geochemistry. Mineralogical Society of America, Washington, DC.

Bruemmer, G.W., J. Gerth, and K.G. Tiller. 1988. Reaction kinetics of the adsorption and desorption of nickel, zinc and cadmium by goethite: I. Adsorption and diffusion of metals. J. Soil Sci. 39:37–52.

Brusseau, M.L., and P.S.C. Rao. 1989. Sorption nonideality during organic contaminant transport in porous media. CRC Crit. Rev. Environ. Control 19:33–99.

Bunnett, J.F. 1986. Kinetics in solution. p.171–250. *In* C.F. Bernasconi (ed.) Investigations of rates and mechanisms of reactions. John Wiley and Sons, New York, NY.

Bunzl, K., W. Schmidt, and B. Sansoni. 1976. Kinetics of ion exchange in soil organic matter. IV. Adsorption and desorption of Pb^{2+}, Cu^{2+}, Zn^{2+}, and Ca^{2+} by peat. J. Soil Sci. 27:32–41.

Carroll, K.M., M.R. Harkness, A.A. Bracco, and R.B. Balcarcel. 1994. Application of a permeant/polymer diffusional model to the desorption of polychlorinated biphenyls from Hudson River sediments. Environ. Sci. Technol. 28:253–258.

Casey, W.H., H.R. Westrich, G.W. Arnold, and J.F. Banfield. 1989. The surface chemistry of dissolving labradorite feldspar. Geochim. Cosmochim. Acta 53:821–832.

Chang, M., S. Wu, and C. Chen. 1997. Diffusion of volatile organic compounds in pressed humic acid disks. Environ. Sci. Technol. 31:2307–2312.

Charlet, L., and A. Manceau. 1992. X-ray absorption spectroscopic study of the sorption of Cr(III) at the oxide-water interface. II: Adsorption, coprecipitation and surface precipitation on ferric hydrous oxides. J. Colloid Interf. Sci. 148:443–458.

Charlet, L., and A. Manceau. 1993. Structure, formation, and reactivity of hydrous oxide particles: Insights from X-ray absorption spectroscopy. p. 117–164. *In* J. Buffle and H.P. van Leeuwen (ed.) Environmental particles. Lewis Publishers, Boca Raton, FL.

Chien, S.H., and W.R. Clayton. 1980. Application of Elovich equation to the kinetics of phosphate release and sorption in soils. Soil Sci. Soc. Am. J. 44:265–268.

Chisholm-Brause, C.J., P.A. O'Day, G.E. Brown, Jr., and G.A. Parks. 1990. Evidence for multinuclear metal-ion complexes at solid/water interfaces from X-ray absorption spectroscopy. Nature 348:528–530.

Chute, J.H., and J.P. Quirk. 1967. Diffusion of potassium from mica-like materials. Nature 213:1156–1157.

Comans, R.N.J., and D.E. Hockley. 1992. Kinetics of cesium sorption on illite. Geochim. Cosmochim. Acta 56:1157–1164.

Connaughton, D.F., J.R. Stedinger, L.W. Lion, and M.L. Shuler. 1993. Description of time-varying desorption kinetics: Release of naphthalene from contaminated soils. Environ. Sci. Technol. 27:2397–2403.

Cornelissen, G., P.C.M. VanNoort, J.R. Parsons, and H.A.J. Govers. 1997. Temperature dependence of slow adsorption and desorption kinetics of organic compounds in sediments. Environ. Sci. Technol. 31:454–460.

Crank, J. 1976. The mathematics of diffusion. Oxford University Press (Clarendon), London, UK.

de la Caillerie, J.B., M. Kermaree, and O. Clause. 1995. Impregnation of γ-alumina with Ni (II) and Co (II) ions at neutral pH: Hydrotalcite-type coprecipitate formation and characterization. J. Am. Chem. Soc. 117:11471–11481.

DiToro, D.M., and L.M. Horzempa. 1982. Reversible and resistant components of PCB adsorption-desorption: Isotherms. Environ. Sci. Technol. 16:594–602.

DiVincenzo, J.P., and D.L. Sparks. 1997. Slow sorption kinetics of pentachlorophenol on soil: Concentration effects. Environ. Sci. Technol. 31:977–983.

Eary, L.E., and D. Rai. 1987. Kinetics of chromium(III) oxidation to chromium (VI) by reaction with manganese dioxide. Environ. Sci. Technol. 21:1187–1193.

Farley, K.J., D.A. Dzombak, and F.M.M. Morel. 1985. A surface precipitation model for the sorption of cations on metal oxides. J. Colloid Interf. Sci. 106:226–242.

Fendorf, S.E., M.J. Eick, P.R. Grossl, and D.L. Sparks. 1997. Arsenate and chromate retention mechanisms on goethite. 1. Surface structure. Environ. Sci. Technol. 31:315–320.

Fendorf, S.E., M. Fendorf, D.L. Sparks, and R. Gronsky. 1992. Inhibitory mechanisms of Cr (III) oxidation by δ-MnO_2. J. Colloid Interf. Sci. 153:37–54.

Fendorf, S.E., G.M. Lamble, M.G. Stapleton, M.J. Kelley, and D.L. Sparks. 1994. Mechanisms of chromium (III) sorption on silica: 1. Cr(III) surface structure derived by extended X-ray absorption fine structure spectroscopy. Environ. Sci. Technol. 28:284–289.

Fendorf, S.E., D.L. Sparks, J. A. Franz, and D.M. Camaioni. 1993. Electron paramagnetic resonance stopped-flow kinetic study of manganese (II) sorption-desorption on birnessite. Soil Sci. Soc. Am. J. 57:57–62.

Fendorf, S.E., and R.J. Zasoski. 1992. Chromium (III) oxidation by γ-MnO_2: I. Characterization. Environ. Sci. Technol. 26:79–85.

Fuller, C.C., J.A. Davis, and G.A. Waychunas. 1993. Surface chemistry of ferrihydrite: Part 2. Kinetics of arsenate adsorption and coprecipitation. Geochim. Cosmochim. Acta 57:2271–2282.

Furrer, G., and W. Stumm. 1986. The coordination chemistry of weathering. I. Dissolution kinetics of γ-Al_2O_3 and BeO. Geochim. Cosmochim. Acta 50:1847–1860.

Gardiner, W.C., Jr. 1969. Rates and mechanisms of chemical reactions. Benjamin, New York, NY.

Grossl, P.R., M.J. Eick, D.L. Sparks, S. Goldberg, and C.C. Ainsworth. 1997. Arsenate and chromate retention mechanisms on goethite. 2. Kinetic evaluation using a pressure-jump relaxation technique. Environ. Sci. Technol. 31:321–326.

Grossl, P.R., and D.L. Sparks. 1995. Evaluation of contaminant ion adsorption/desorption on goethite using pressure-jump relaxation kinetics. Geoderma 67:87–101.

Grossl, P.R., D.L. Sparks, and C.C. Ainsworth. 1994. Rapid kinetics of Cu (II) adsorption/desorption on goethite. Environ. Sci. Technol. 28:1422–1429.

Hachiya, K., M. Sasaki, I. Ikeda, N. Mikami, and T. Yasunaga. 1984. Static and kinetic studies of adsorption-desorption of metal ions on a γ-Al_2O_3 surface. 2. Kinetic studies by means of pressure-jump technique. J. Phys. Chem. 88:27–31.

Hamaker, J.W., and J.M. Thompson. 1972. Adsorption. p. 39–151. *In* C.A.I. Goring and J.W. Hamaker (ed.) Organic chemicals in the environment, Marcel Dekker, New York, NY.

Harmon, T.C., L. Semprini, and P.V. Roberts. 1992. Simulating solute transport using laboratory-based sorption parameters. J. Environ. Eng. 118:666–689.

Havlin, J.L., and D.G. Westfall. 1985. Potassium release kinetics and plant response in calcareous soils. Soil Sci. Soc. Am. J. 49:366–370.

Hayes, K.F., and J.O. Leckie. 1986. Mechanism of lead ion adsorption at the goethite-water interface. ACS Symp. Ser. 323:114–141.

Hellman, R., B. Drake, and K. Kjoller. 1992. Using atomic force microscopy to study the structure, topography and dissolution of albite surfaces. p. 149–152. *In* Y.K. Kharaka and A.S. Maest (ed.) Water-rock interaction VIIA. A. Balkema, Rotterdam, Netherlands.

Hem, J.D. 1978. Redox processes at the surface of manganese oxide and their effects on aqueous metal ions. Chem. Geol. 21:199–218.

Hillner, P.E., A.J. Gratz, S. Manne, and P.K. Hansma. 1992a. Atomic-scale imaging of calcite growth and dissolution in real-time. Geol. 20:359–362.

Hillner, P.E., S. Manne, A.J. Gratz, and P.K. Hansma. 1992b. AFM images of dissolution and growth on a calcite crystal. Ultramicrosc. 44:1387–1393.

Huang, P.M. 1991. Kinetics of redox reactions on manganese oxides and its impact on environmental quality. p. 191–230. *In* D.L. Sparks and D.L. Suarez (ed.) Rates of soil chemical processes. Soil Science Society of America, Madison, WI.

Jardine, P.M., F.M. Dunnivant, H.M. Selim, and J.F. McCarthy. 1992. Comparison of models for describing the transport of dissolved organic carbon in aquifer columns. Soil Sci. Soc. Am. J. 56:393–401.

Jardine, P.M., G.K. Jacobs, and J.D. O'Dell. 1993. Unsaturated transport processes in undisturbed heterogeneous porous media: II. Co-contaminants. Soil Sci. Soc. Am. J. 57:954–962.

Jardine, P.M., and D.L. Sparks. 1984. Potassium-calcium exchange in a multireactive soil system. I. Kinetics. Soil Sci. Soc. Am. J. 48:39–45.

Johnsson, P.A., M.F. Hochella, Jr., G.A. Parks, A.E. Blum, and G. Sposito. 1992. Direct observation of muscovite basal-plane dissolution and secondary phase formation: An XPS, LEED, and SFM study. p. 159–162. *In* Y.K. Kharaka and A.S. Maest (ed.) Water-rock interaction VIIA. A. Balkema, Rotterdam, Netherlands.

Jordan, G., and W. Rammensee. 1996. Dissolution rates and activation energy for dissolution of brucite (001): A new method based on the microtopography of crystal surfaces. Geochim. Cosmochim. Acta 60:5055–5062.

Junta, J.L., and M.F. Hochella, Jr. 1994. Manganese (II) oxidation at mineral surfaces: A microscopic and spectroscopic study. Geochim. Cosmochim. Acta 58:4985–4999.

Kan, A.T., G. Fu, M.A. Hunter, and M.B. Tomson. 1997. Irreversible adsorption of napthalene and tetrachlorobiphenyl to Lula and surrogate sediments. Environ. Sci. Technol. 31:2176–2185.

Karickhoff, S.W. 1980. Sorption kinetics of hydrophobic pollutants in natural sediments. p. 193–205. *In* R.A. Baker (ed.) Contaminants and sediments. 2. Ann Arbor Science, Ann Arbor, MI.

Karickhoff, S.W., D.S. Brown, and T.A. Scott. 1979. Sorption of hydrophobic pollutants on natural sediments. Water Res. 13:241–248.

Karickhoff, S.W., and K.R. Morris. 1985. Sorption dynamics of hydrophobic pollutants in sediment suspensions. Environ. Toxicol. Chem. 4:469–479.

Keren, R., P.R. Grossl, and D.L. Sparks. 1994. Equilibrium and kinetics of borate adsorption-desorption on pyrophyllite in aqueous suspensions. Soil Sci. Soc. Am. J. 58:1116–1122.

Krishnamurti, G.S.R., and P.M. Huang. 1992. Dynamics of potassium chloride induced manganese release in different soil orders. Soil Sci. Soc. Am. J. 56:1115–1123.

Krishnamurti, G.S.R., G. Cieslinski, P.M. Huang, and K.C.J. Van Rees. 1997. Kinetics of cadmium release from soils as influenced by organic acids: Implication in cadmium availability. J. Environ. Qual. 26:271–277.

Kuo, S., and E.G. Lotse. 1974. Kinetics of phosphate adsorption and desorption by lake sediments. Soil Sci. Soc. Am. Proc. 38:50–54.

Kuo, S., and D.S. Mikkelsen. 1980. Kinetics of zinc desorption from soils. Plant Soil 56:355–364.

Lasaga, A.C. 1984. Chemical kinetics of water-rock interactions. J. Geophys. Res. B 6:4009–4025.

Lee, L.S., P.S.C. Rao, M.L. Brusseau, and R.A. Ogwada. 1988. Nonequilibrium sorption of organic contaminants during flow through columns of aquifer materials. Environ. Toxicol. Chem. 7:779–793.

Leenheer, J.A., and J.L. Ahlrichs. 1971. A kinetic and equilibrium study of the adsorption of carbaryl and parathion upon soil organic matter surfaces. Soil Sci. Soc. Am. Proc. 35:700–704.

Lehmann, R.G., and R.D. Harter. 1984. Assessment of copper-soil bond strength by desorption kinetics. Soil Sci. Soc. Am. J. 48:769–772.

Loehr, R.C., and M.T. Webster. 1996. Behavior of fresh vs. aged chemicals in soils. J. Soil Contam. 5:361–383.

Lövgren, L., S. Sjöberg, and P.W. Schindler. 1990. Acid/base reactions and Al(III) complexation at the surface of goethite. Geochim. Cosmochim. Acta. 54:1301–1306.

Low, M.J.D. 1960. Kinetics of chemisorption of gases on solids. Chem. Rev. 60: 267–312.

Maurice, P.A. 1997. Scanning probe microscopy of mineral surfaces. *In* P.M. Huang, N. Senesi and J. Buffle (ed.) Structure and surface reactions of soil particles. Vol. 4. John Wiley and Sons, New York, NY.

Maurice, P.A., M.F. Hochella, Jr., G.A. Parks, G. Sposito, and U. Schwertmann. 1995. Evolution of hematite surface microtopography upon dissolution by simple organic acids. Clays Clay Miner. 43:29–38.

McCall, P.J., and G.L. Agin. 1985. Desorption kinetics of picloram as affected by residence time in the soil. Environ. Toxicol. Chem. 4:37–44.

Mikami, N., M. Sasaki, K. Hachiya, R.D. Ikeda, and T. Yasunaga. 1983a. Kinetics of the adsorption of PO_4 on the γ-Al_2O_3 surface using the pressure-jump technique. J. Phys. Chem. 87:1454–1458.

Mikami, N., M. Sasaki, T. Kikuchi, and T. Yasunaga. 1983b. Kinetics of the adsorption-desorption of chromate on γ-Al_2O_3 surfaces using the pressure-jump technique. J. Phys. Chem. 87:5245–5248.

Mikami, N., M. Sasaki, K. Hachiya, and T. Yasunaga. 1983c. Kinetic study of the adsorption-desorption of the uranyl ion on a γ-Al_2O_3 surface using the pressure-jump technique. J. Phys. Chem. 87:5478–5481.

Miller, C.T., and J. Pedit. 1992. Use of a reactive surface-diffusion model to describe apparent sorption-desorption hysteresis and abiotic degradation of lindane in a subsurface material. Environ. Sci. Technol. 26:1417–1427.

Murray, J.W., and J.G. Dillard. 1979. The oxidation of cobalt (II) adsorbed on manganese dioxide. Geochim. Cosmochim. Acta 43:781–787.

Nkedi-Kizza, P., J.W. Biggar, H.M. Selim, M.T. van Genuchten, P.J. Wierenga, J.M. Davidson, and D.R. Nielsen. 1984. On the equivalence of two conceptual models for describing ion exchange during transport through an aggregated Oxisol. Water Resour. Res. 20:1123–1130.

O'Day, P.A., G.A. Parks, and G.E. Brown, Jr. 1994a. Molecular structure and binding sites of cobalt(II) surface complexes on kaolinite from X-ray absorption spectroscopy. Clays Clay Miner. 42:337–355.

O'Day, P.A., G.E. Brown, Jr., and G.A. Parks. 1994b. X-ray absorption spectroscopy of cobalt (II) multinuclear surface complexes and surface precipitates on kaolinite. J. Coll. Interf. Sci. 165:269–289.

O'Day, P.A., C.J. Chisholm-Brause, S.N. Towle, G.A. Parks, and G.E. Brown, Jr. 1996. X-ray absorption spectroscopy of Co(II) sorption complexes on quartz (α-SiO_2) and rutile (TiO_2). Geochim. Cosmochim. Acta. 60:2515–2532.

Onken, A.B., and R.L. Matheson. 1982. Dissolution rate of EDTA-extractable phosphate from soils. Soil Sci. Soc. Am. J. 46:276–279.

Oscarson, D.W., P.M. Huang, C. Defosse, and A. Herbillon. 1981. The oxidative power of Mn (IV) and Fe (III) oxides with respect to As (III) in the terrestrial and aquatic environment. Nature 291:50–51.

Oscarson, D.W., P.M. Huang, and U.T. Hammer. 1983. Oxidation and sorption of arsenite by manganese dioxide as influenced by surface coatings of iron and aluminum oxides and calcium carbonate. Water Air Soil Pollut. 20:233–244.

Oscarson, D.W., P.M. Huang, and W.K. Liaw. 1980. The oxidation of arsenite by aquatic sediments. J. Environ. Qual. 9:700–703.

Padmanabham, M. 1983. Adsorption-desorption behavior of copper (II) at the goethite-solution interface. Aust. J. Soil Res. 21:309–320.

Pavlostathis, S.G., and G.N. Mathavan. 1992. Desorption kinetics of selected volatile organic compounds from field contaminated soils. Environ. Sci. Technol. 26:532–538.

Pedit, J.A., and C.T. Miller. 1995. Heterogenous sorption processes in subsurface systems. 2. Diffusion modeling approaches. Environ. Sci. Technol. 29:1766–1772.

Petrovic, R., R.A. Berner, and M.B. Goldhaber. 1976. Rate control in dissolution of alkali feldspars. I. Study of residual feldspar grains by X-ray photoelectron spectroscopy. Geochim. Cosmochim. Acta 40:537–548.

Pignatello, J.J., F.J. Ferrandino, and L.Q. Huang. 1993. Elution of aged and freshly added herbicides from a soil. Environ. Sci. Technol. 27:1563–1571.

Pignatello, J.J., and L.Q. Huang. 1991. Sorptive reversibility of atrazine and metolachlor residues in field soil samples. J. Environ. Qual. 20:222–228.

Polyzopoulos, N.A., V.Z. Keramidas, and A. Pavlatou. 1986. On the limitations of the simplified Elovich equation in describing the kinetics of phosphate sorption and release from soils. J. Soil Sci. 37:81–87.

Rai, E., and R.J. Serne. 1977. Plutonium activities in soil solutions and the stability and formation of selected plutonium minerals. J. Environ. Qual. 6:89–95.

Scheidegger, A.M., G.M. Lamble, and D.L. Sparks. 1996. Investigation of Ni sorption on pyrophyllite: An XAFS study. Environ. Sci. Technol. 30:548–554.

Scheidegger, A.M., and D.L. Sparks. 1996a. Kinetics of the formation and the dissolution of nickel surface precipitates on pyrophyllite. Chem. Geol. 132:157–164.

Scheidegger, A.M., and D.L. Sparks. 1996b. A critical assessment of sorption-desorption mechanisms at the soil mineral/water interface. Soil Sci. 161:813–831.

Scheidegger, A.M., G.M. Lamble, and D.L. Sparks. 1997. Spectroscopic evidence for the formation of mixed-cation hydroxide phases upon metal sorption on clays and aluminum oxides. J. Colloid Interf. Sci. 186:118–128.

Scheidegger, A.M., D.G. Strawn, G.M. Lamble, and D.L. Sparks. 1998. The kinetics of mixed Ni-Al hydroxide formation on clays and aluminum oxide: A time-resolved XAFS study. Geochim. Cosmochim. Acta.62:2233–2245.

Schott, J., and J.C. Petit. 1987. New evidence for the mechanisms of dissolution of silicate minerals. p. 293–312. *In* W. Stumm (ed.) Aquatic surface chemistry, John Wiley and Sons, New York, NY.

Schultz, M.F., M.M. Benjamin, and J.F. Ferguson. 1987. Adsorption and desorption of metals on ferrihydrite: Reversibility of the reaction and sorption properties of the regenerated solid. Environ. Sci. Technol. 21:863–869.

Schwarzenbach, R.T., P.M. Gschwend, and D.M. Boden. 1993. Environmental organic chemistry. John Wiley and Sons, New York , NY.

Scott, M.J., and J.J. Morgan. 1995. Reactions at oxide surfaces. 1. Oxidation of As (III) by synthetic birnessite. Environ. Sci. Technol. 29:1898–1905.

Scott, M.J., and J.J. Morgan. 1996. Reactions at oxide surfaces. 2. Oxidation of Se(IV) by synthetic birnessite. Environ. Sci. Technol. 30:1990–1996.

Scribner, S.L., T.R. Benzing, S. Sun, and S.A. Boyd. 1992. Desorption and bioavailability of aged simazine residues in soil from a continuous corn field. J. Environ. Qual. 21:115–120.

Sharpley, A.N. 1983. Effect of soil properties on the kinetics of phosphorus desorption. Soil Sci. Soc. Am. J. 47:462–467.

Skopp, J. 1986. Analysis of time dependent chemical processes in soils. J. Environ. Qual. 15:205–213.

Sparks, D.L. 1989. Kinetics of soil chemical processes. Academic Press, San Diego, CA.

Sparks, D.L. 1991. Chemical kinetics and mass transfer processes in soils and soil constituents. p. 585–637. *In* J. Bear and M.Y. Corapcioglu (ed.) Transport processes in porous media. Kluwer Academic Publishers, Dordecht, Netherlands.

Sparks, D.L. 1995. Environmental soil chemistry. Academic Press, San Diego, CA.

Sparks, D.L. 1998. Kinetics of sorption/release processes on natural surfaces. *In* P.M. Huang, N. Senesi, and J. Buffle (ed.) Structure and surface reaction of soil particles. Vol. 4. John Wiley and Sons, New York, NY.

Sparks, D.L. 1999. Kinetics of soil chemical phenomena: Future directions. p. 81–102. *In* P.M. Huang, D.L. Sparks, and S.A. Boyd (ed). Future prospects for soil chemistry. Soil Sci. Soc. Am. Spec. Pub., Soil Science Society of America, Madison, WI.

Sparks, D.L., and P.M. Jardine. 1984. Comparison of kinetic equations to describe K-Ca exchange in pure and in mixed systems. Soil Sci. 138:115–122.

Sparks, D.L., and D.L. Suarez (eds). 1991. Rates of soil chemical processes. Soil Sci. Soc. Am. Spec. Pub. 27, Soil Science Society of America, Madison, WI.

Sparks, D.L., and P.C. Zhang. 1991. Relaxation methods for studying kinetics of soil chemical phenomena. p. 61–94. *In* D.L. Sparks, and D.L. Suarez (eds.) Rates of soil chemical processes. Soil Sci. Soc. Am. Spec. Pub. 27, Soil Science Society of America, Madison, WI.

Sparks, D.L., S.E. Fendorf, P.C. Zhang, and L. Tang. 1993. Kinetics and mechanisms of environmentally important reactions on soil colloidal surfaces. p. 141–168. *In* D. Petruzzelli and F.G. Helfferich (ed.) Migration and fate of pollutants in soils and subsoils. Springer-Verlag, Berlin, Germany.

Sparks, D.L., S.E. Fendorf, C.V. Toner, IV, and T.H. Carski. 1996. Kinetic methods and measurements. p. 1275–1307. *In* D.L. Sparks (ed.) Methods of soil analysis. Part 3. Chemical methods. Soil Science Society of America, Madison, WI.

Sposito, G. 1986. Distinguishing adsorption from surface precipitation. ACS Symp. Ser. 323:217–228.

Sposito, G. 1994. Chemical equilibria and kinetics in soils. John Wiley and Sons, New York, NY.

Steinberg, S.M., J.J. Pignatello, and B.L. Sawhney. 1987. Persistence of 1,2 dibromoethane in soils: Entrapment in intra particle micropores. Environ. Sci. Technol. 21:1201–1208.

Stone, A.T. 1986. Adsorption of organic reductants and subsequent electron transfer on metal oxide surfaces. ACS Symp. Ser. 323:446–461.

Stone, A.T. 1987a. Microbial metabolites and the reductive dissolution of manganese oxides: Oxalate and pyruvate. Geochim. Cosmochim. Acta 51:919–925.

Stone, A.T. 1987b. Reductive dissolution of manganese (III/IV) oxides by substituted phenols. Environ. Sci. Technol. 21:979–988.

Stone, A.T. 1991. Oxidation and hydolysis of ionizable organic pollutants at hydrous metal oxide surfaces. p. 231–254. *In* D.L. Sparks and D.L. Suarez (ed.) Rates of soil chemical processes. Soil Sci. Soc. Am. Spec. Pub. 27, Soil Science Society of America, Madison, WI.

Stone, A.T., and J.J. Morgan. 1984a. Reduction and dissolution of manganese (III) and manganese (IV) oxides by organics. 1. Reaction with hydroquinone. Environ. Sci. Technol. 18:450–456.

Stone, A.T., and J.J. Morgan. 1984b. Reduction and dissolution of manganese (III) and manganese (IV) oxides by organics. 2. Survey of the reactivity of organics. Environ. Sci. Technol. 18:617–624.

Stumm, W. 1992. Chemistry of the solid-water interface. John Wiley and Sons, New York, NY.

Stumm, W., and G. Furrer. 1987. The dissolution of oxides and aluminum silicates: Examples of surface-coordination-controlled kinetics. p. 197–219. *In* W. Stumm (ed.) Aquatic surface chemistry, John Wiley and Sons, New York, NY.

Stumm, W., and R. Wollast. 1990. Coordination chemistry of weathering. Kinetics of the surface-controlled dissolution of oxide minerals. Rev. Geophys. 28:53–69.

Takahashi, M.T., and R.A. Alberty. 1969. The pressure-jump methods. p. 31–55. *In* K. Kustin (ed.) Methods in enzymology 16. Academic Press, New York, NY.

Tang, L., and D.L. Sparks. 1993. Cation exchange kinetics on montmorillonite using pressure-jump relaxation. Soil Sci. Soc. Am. J. 57:42–46.

Toner IV, C.V., and D.L. Sparks. 1995. Chemical relaxation and double layer model analysis of boron adsorption on alumina. Soil Sci. Soc. Am. J. 59:395–404.

Towle, S.N., J.R. Bargar, G.E. Brown, Jr., and G.A. Parks. 1997. Surface precipitation of Co(II) (aq) on Al_2O_3. J. Colloid Interf. Sci. 187:62–82.

van Genuchten, M.T., and R.J. Wagenet. 1989. Two-site/two-region models for pesticide transport and degradation: Theoretical development and analytical solutions. Soil Sci. Soc. Am. J. 53:1303–1310.

Waychunas, G.A., B.A. Rea, C.C. Fuller, and J.A. Davis. 1993. Surface chemistry of ferrihydrite: Part 1. EXAFS studies of the geometry of coprecipitated and adsorbed arsenate. Geochim. Cosmochim. Acta 57:2251–2269.

Weber, W.J., Jr., and J.P. Gould. 1966. Sorption of organic pesticides from aqueous solution. Adv. Chem. Ser. 60:280–305.

Weber, W.J., Jr., and C.T. Miller. 1988. Modeling the sorption of hydrophobic contaminants by aquifer materials. 1. Rates and equilibria. Water Res. 22:457–464.

Weber, W.J., Jr., and W. Huang. 1996. A distributed reactivity model for sorption by soils and sediments. 4. Intraparticle heterogeneity and phase-distribution relationships under nonequilibrium conditions. Environ. Sci. Technol. 30:881–888.

Wersin, P., M.F. Hochella, Jr., P. Persson, G. Redden, J.O. Leckie, and D.W. Harris. 1994. Interaction between aqueous uranium (VI) and sulfide minerals: Spectroscopic evidence for sorption and reduction. Geochim. Cosmochim. Acta 58:2829–2843.

Werth, C.J., and M. Reinhard. 1997. Effects of temperature on trichloroethylene desorption from silica gel and natural sediments. 2. Kinetics. Environ. Sci. Technol. 31:697–703.

Wollast, R. 1967. Kinetics of the alteration of K-feldspar in buffered solutions at low temperature. Geochim. Cosmochim. Acta 31:635–648.

Wu, S., and P.M. Gschwend. 1986. Sorption kinetics of hydrophobic organic compounds to natural sediments and soils. Environ. Sci. Technol. 20:717–725.

Xia, K., A. Mehadi, R.W. Taylor, and W.F. Bleam. 1997. X-ray absorption and electron paramagnetic resonance studies of Cu(II) sorbed to silica: Surface-induced precipitation at low surface coverages. J. Coll. Interf. Sci. 185:252–257.

Xu, J., and P.M. Huang. 1995. Zinc adsorption-desorption on short-range ordered iron oxide as influenced by citric acid during its formation. Geoderma 64:232–356.

Xue, Y., and S.J. Traina. 1996. Oxidation kinetics of Co (II) - EDTA in aqueous and semi-aqueous goethite suspensions. Environ. Sci. Technol. 30:1975–1981.

Zhang, P.C., and D.L. Sparks. 1989. Kinetics and mechanisms of molybdate adsorption/desorption at the goethite/water interface using pressure-jump relaxation. Soil Sci. Soc. Am. J. 53:1028–1034.

Zhang, P.C., and D.L. Sparks. 1990a. Kinetics and mechanisms of sulfate adsorption/desorption on goethite using pressure-jump relaxation. Soil Sci. Soc. Am. J. 54:1266–1273.

Zhang, P.C., and D.L. Sparks. 1990b. Kinetics of selenate and selenite adsorption/desorption at the goethite/water interface. Environ. Sci. Technol. 24:1848–1856.

Zinder, B., G. Furrer, and W. Stumm. 1986. The coordination chemistry of weathering. II. Dissolution of Fe(III) oxides. Geochim. Cosmochim. Acta 50:1861–1869.